

Training Sequence Design for Feedback Assisted Hybrid Beamforming in Massive MIMO Systems

Song Noh, Michael D. Zoltowski, and David J. Love

Abstract—Large-scale antenna systems are an emerging technology that uses an excess of transmit antennas to realize high spectral and energy efficiency for future wireless networks. Obtaining potential gains from using large-scale antenna arrays in practical systems hinges on sufficient levels of channel estimation accuracy. Most prior work focused on a cellular network based on TDD operation that relies on channel reciprocity between uplink and downlink channels, whereas most current wireless systems are based on FDD operation without channel reciprocity, where the problem of channel estimation becomes more challenging due to substantial training resources and feedback overheads that scales with the number of antennas. In this paper, we consider the problem of training sequence design that specifies a set of training signals and its mapping to the training periods. The proposed training sequence is designed to minimize the steady-state channel estimation performance by exploiting signal-to-noise ratio (SNR) and the spatio-temporal channel statistics in conjunction with Kalman filtering. In addition, we focus on a reduced dimensionality training sequence and transmit precoding design aimed at reducing hardware complexity and power consumption, which extends to hybrid analog-digital precoding scheme that uses a limited number of active RF chains for transmit precoding by applying the Toeplitz distribution theorem to large-scale linear antenna arrays. A practical guideline for training sequence parameters is presented with performance analysis. Numerical results show the effectiveness of the proposed algorithm.

Index Terms—Massive MIMO systems, channel estimation, training sequence design, hybrid beamforming

I. INTRODUCTION

Multiple-input multiple-output (MIMO) technologies have been shown to be effective to provide reliable wireless links and the advantages of MIMO communications are widely recognized [2]. MIMO systems utilizing a large-scale antenna array at the base station, so called *massive MIMO* systems, are emerging as key technologies for the design of throughput and energy efficient systems for future wireless communications. Massive MIMO represents a paradigm shift in system configuration in that each antenna element uses extremely low power to perform simple signal processing such as spatial matched filtering [3] by exploiting favorable assumptions about the propagation environment that arise from asymptotic random matrix analysis. Because the large size of the transmit antenna array relative to the number of serviced users can mitigate thermal noise, fast

channel fading, and some interference, from the law of large numbers [3], [4].

However, the potential gains of massive MIMO in practical systems are limited by channel estimation accuracy [5]. In contrast to current MIMO systems equipped with a few antennas at each base station, the training signal overhead required for channel estimation in a massive MIMO system can be overwhelming, since the number of time slots for transmitting orthogonal training signals must be at least as large as the number of antennas. In addition, an important issue regarding the cost of implementation is that the number of active RF chains required for channel sounding and transmit precoding are limited relative to the number of antennas [2]. As a result, channel estimation schemes that are reliable and require a low training overhead and low-complexity are important in order to efficiently utilize the large antenna array gains.

To tackle the challenge of channel estimation, much of the prior work focused on time-division duplex (TDD) operation assuming channel reciprocity [3], [4], [6] to acquire channel state information (CSI) at the base station under the assumption of time-invariant channels within the coherence time. In a TDD mode, the uplink channel sounding enables downlink channel estimation by using channel reciprocity that requires proper calibration of the hardware chains between the terminal uplink and downlink chains [7]. In addition, in multi-cell environment with a high frequency reuse factor, pilot contamination induced by use of non-orthogonal uplink training signal in neighboring cells leads to imperfect channel estimation which causes severely degraded system performance [5].

In most wireless systems that employ a frequency-division duplex (FDD) mode, the problem of channel estimation becomes more challenging because downlink channel estimation requires substantial overhead, such as feedback and dedicated times for channel sounding which scales with the number of antennas. Recently, initial work on the design of FDD massive MIMO systems considered pilot beam pattern design, feedback technique, and spatial division multiplexing [8]–[15]. In an FDD mode, it was shown that the overhead for channel estimation does not scale with the number of antennas in conjunction with underlying channel statistics and a specific antenna arrangement.

In this paper, we consider the design of a training scheme that properly specifies the training signals and its mapping to the corresponding training phase for downlink channel estimation in FDD massive MIMO systems. We refer to this scheme as using a *training sequence*. Under a Kalman

S. Noh, M. Zoltowski, and D. J. Love are with the School of Electrical and Computer Engineering, Purdue University, West Lafayette, IN 47907, USA (e-mail: songnoh@purdue.edu and {mikedz,djlove}@ecn.purdue.edu). A preliminary version of this work will be presented in [1].

filtering framework, the proposed training sequence is designed to minimize the steady-state channel mean square error (MSE) to leverage channel estimation performance. In addition, we focus on a reduced-dimensionality training sequence and transmit precoding design aimed at reducing the cost of implementation and power consumption [2]. We then extend the low-dimensional constraint to hybrid analog-digital precoding scheme that uses a limited number of available RF chains for digital baseband precoding by applying the Toeplitz distribution theorem to an uniformly spaced linear array (ULA) at the base station. For performance analysis, we adopt *deterministic equivalent* technique [6] to handle the case of large antenna arrays and provide a practical guideline for training sequence parameters.

This paper is organized as follows. The system model and background are described in Section II. Section III describes the proposed training sequence and hybrid analog-digital precoding design. In Section IV, an extension to multi-user massive MIMO systems is discussed with performance analysis. Numerical results are provided in Section V, followed by conclusions in Section VI.

Notations: Vectors and matrices are written in boldface with matrices in capitals. All vectors are column vectors. For a matrix \mathbf{A} , \mathbf{A}^T , \mathbf{A}^H , and $\text{tr}(\mathbf{A})$ indicate the transpose, Hermitian transpose, and trace of \mathbf{A} , respectively. $\mathbf{A} \odot \mathbf{B}$ denotes the Hadamard product between \mathbf{A} and \mathbf{B} . $\mathbf{A}_{\mathcal{I}}$ is a submatrix of \mathbf{A} composed of the column vectors of the index set \mathcal{I} . $[\mathbf{A}]_{p,q}$ represents the element in the p -th row and the q -th column of \mathbf{A} . $\text{diag}(d_1, \dots, d_n)$ is the diagonal matrix composed of elements d_1, \dots, d_n . \mathbf{I}_N stands for the identity matrix of size N ; $\mathbf{1}_{M \times N}$ and $\mathbf{0}_{M \times N}$ denote an $M \times N$ matrix composed of all-ones and all-zeros, respectively. For a vector \mathbf{a} , $\|\mathbf{a}\|_p$ represents the p -norm. For a matrix \mathbf{A} , $\|\mathbf{A}\|_F$ denotes the Frobenious norm. $\mathbf{x} \sim \mathcal{CN}(\boldsymbol{\mu}, \boldsymbol{\Sigma})$ means that random vector \mathbf{x} is complex Gaussian distributed with mean $\boldsymbol{\mu}$ and covariance matrix $\boldsymbol{\Sigma}$. $E\{\cdot\}$ denotes statistical expectation. \mathbb{N} and \mathbb{C} denote the set of natural numbers and complex numbers, respectively.

II. SYSTEM MODEL

We consider a massive MIMO system with N_t transmit antennas and a single receive antenna over flat Rayleigh-fading channels, as shown in Fig. 1. We focus on the single user case first and then point out the multiple-user case in Section IV. We assume block transmission with M consecutive symbols for one block composed of a pilot transmission period of M_p symbols and a data transmission period of M_d symbols, i.e., $(M = M_p + M_d)$. The received signal at the k -th symbol time is given by

$$y_k = \mathbf{h}_\ell^H \mathbf{s}_k + w_k, \quad \text{for } k = \ell M + m, \quad (1)$$

where $\ell = 0, 1, \dots$ and $1 \leq m \leq M$ so that $k = 1, 2, \dots$. Here, $\mathbf{s}_k \in \mathbb{C}^{N_t}$ is the transmitted symbol vector with power constraint $E\{\|\mathbf{s}_k\|_2^2\} = \rho$ and $\mathbf{h}_\ell \in \mathbb{C}^{N_t}$ is the channel vector with additive noise $w_k \sim \mathcal{CN}(0, 1)$. The transmit vector \mathbf{s}_k represents a training signal vector during the

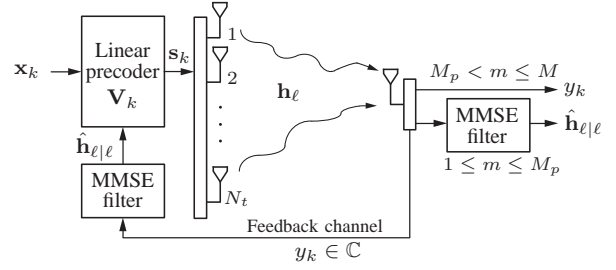


Fig. 1. Massive MIMO system model for the symbol time $k = \ell M + m$

training period (i.e., $k = \ell M + m$ where $1 \leq m \leq M_p$). On the other hand, during the data transmission phase ($M_p < m \leq M$), \mathbf{s}_k denotes a precoded data vector constructed by mapping the data symbols $\mathbf{x}_k = [x_{1,k}, \dots, x_{U,k}]^T \in \mathbb{C}^U$ to the transmit antenna array using the multi-dimensional beamformer $\mathbf{V}_k \in \mathbb{C}^{N_t \times U}$, i.e., $\mathbf{s}_k = \mathbf{V}_k \mathbf{x}_k$. We first consider a single data stream transmission ($U = 1$) in which a rank-one beamformer is denoted as $\mathbf{v}_k \in \mathbb{C}^{N_t}$, and then extend to the case of $U > 1$.

We assume that the channel is block-fading and that the channel remains constant during each of the ℓ -th transmission blocks in (1). The channel temporal variation across the blocks is modeled using a state-space framework as a first-order stationary Gauss-Markov process [16] with

$$\mathbf{h}_{\ell+1} = a\mathbf{h}_\ell + \sqrt{1 - a^2}\mathbf{b}_{\ell+1}, \quad (2)$$

where $a \in (0, 1)$ denotes the temporal fading correlation coefficient, \mathbf{b}_ℓ denotes process noise for the ℓ -th block time index where $\mathbf{b}_\ell \sim \mathcal{CN}(\mathbf{0}, \mathbf{R}_h)$, and the channel spatial correlation is given by $\mathbf{R}_h = E\{\mathbf{h}_\ell \mathbf{h}_\ell^H\}$ for all ℓ . The channel model can represent a spatially correlated channel by considering $\text{rank}(\mathbf{R}_h) = r$ where $r \leq N_t$. An eigen-decomposition (ED) of \mathbf{R}_h is given by

$$\mathbf{R}_h = \mathbf{U} \boldsymbol{\Lambda} \mathbf{U}^H, \quad (3)$$

where $\mathbf{U} = [\mathbf{u}_1, \dots, \mathbf{u}_r] \in \mathbb{C}^{N_t \times r}$ and $\boldsymbol{\Lambda} = \text{diag}(\lambda_1, \dots, \lambda_r)$ composed of the non-zero eigenvalues of \mathbf{R}_h in descending order. Throughout the paper, we assume that the channel statistics (a, \mathbf{R}_h) are known to the system.¹

During the ℓ -th training period, the received signal model (1) can be rewritten in vector form as

$$\mathbf{y}_{\ell, \text{pilot}} = \mathbf{S}_\ell^H \mathbf{h}_\ell + \mathbf{w}_\ell, \quad (4)$$

where $\mathbf{S}_\ell = [\mathbf{s}_{\ell M+1} \dots \mathbf{s}_{\ell M+M_p}]$ denotes the transmitted training signals subject to an average transmit power constraint $E\{\|\mathbf{S}_\ell\|_F^2\} = \rho M_p$, $\mathbf{y}_{\ell, \text{pilot}} = [y_{\ell M+1}, \dots, y_{\ell M+M_p}]^H$, and \mathbf{w}_ℓ is similarly defined. We focus on minimum mean square error (MMSE) channel estimation based on the current and all previous received training signals given by $\hat{\mathbf{h}}_{\ell|l} = E\{\mathbf{h}_\ell | \mathbf{y}_{\text{pilot}}^{(\ell)}\}$, where $\mathbf{y}_{\text{pilot}}^{(\ell)} = \{\mathbf{y}_{\ell', \text{pilot}} | \ell' \leq \ell\}$ denotes all received training signals up to the ℓ -th training period. From (2) and (4), the system can be viewed as a state-space model, and then

¹Please see [9] for a discussion of a practical estimation approach in massive MIMO systems.

optimal channel estimation is given by Kalman filtering, as shown in Table I. Here, $(\mathbf{P}_{\ell|\ell}, \mathbf{P}_{\ell|\ell-1})$ are the estimation and prediction error covariance matrices and \mathbf{K}_ℓ denotes the Kalman gain matrix, defined as

$$\begin{aligned}\mathbf{P}_{\ell|\ell'} &= E\{(\mathbf{h}_\ell - \hat{\mathbf{h}}_{\ell|\ell'}) (\mathbf{h}_\ell - \hat{\mathbf{h}}_{\ell|\ell'})^H | \mathbf{y}_{pilot}^{(\ell')}\} \\ \mathbf{K}_\ell &= \mathbf{P}_{\ell|\ell-1} \mathbf{S}_\ell (\mathbf{S}_\ell^H \mathbf{P}_{\ell|\ell-1} \mathbf{S}_\ell + \mathbf{I}_{M_p})^{-1}.\end{aligned}$$

Initialization:

$$\hat{\mathbf{h}}_{0|-1} = \mathbf{0} \quad \text{and} \quad \mathbf{P}_{0|-1} = \mathbf{R}_h \quad (5)$$

while $\ell = 0, 1, \dots$ **do**

Measurement update:

$$\hat{\mathbf{h}}_{\ell|\ell} = \hat{\mathbf{h}}_{\ell|\ell-1} + \mathbf{K}_\ell (\mathbf{y}_{\ell, pilot} - \mathbf{S}_\ell^H \hat{\mathbf{h}}_{\ell|\ell-1}) \quad (6)$$

$$\mathbf{P}_{\ell|\ell} = \mathbf{P}_{\ell|\ell-1} - \mathbf{K}_\ell \mathbf{S}_\ell^H \mathbf{P}_{\ell|\ell-1} \quad (7)$$

Time update:

$$\begin{aligned}\hat{\mathbf{h}}_{\ell+1|\ell} &= a \hat{\mathbf{h}}_{\ell|\ell} \\ \mathbf{P}_{\ell+1|\ell} &= a^2 \mathbf{P}_{\ell|\ell} + (1 - a^2) \mathbf{R}_h\end{aligned} \quad (8)$$

end while

TABLE I
CHANNEL ESTIMATION BASED ON KALMAN FILTERING [17]

In this paper, we employ the concept of a *training frame*. A training frame is the joint design of the training signals sent over G consecutive blocks. This means for each i , $\mathbf{S}_{iG}, \mathbf{S}_{iG+1}, \dots, \mathbf{S}_{(i+1)G-1}$ are jointly designed. We assume $G = 2^s$ for $s \in \{0, 1, 2, \dots\}$ for simplicity, which will be revisited later.

During the ℓ -th data transmission period (i.e., channels uses satisfying $k = \ell M + m$ with $M_p < m \leq M$), we assume that the data symbol x_k is transmitted with a rank-one beamformer $\mathbf{v}_k \in \mathbb{C}^{N_t}$. To realize a low-complexity solution for the beamformer design, we assume the beamformer \mathbf{v}_k is restricted to a subspace of dimension n_d which should be optimized to meet the effective channel rank. Then, we can write \mathbf{v}_k as a hybrid beamforming $\mathbf{v}_k = \mathbf{F} \mathbf{d}_k$, i.e., \mathbf{v}_k lies in column space of $\mathbf{F} \in \mathbb{C}^{N_t \times n_d}$ with its linear combination of $\mathbf{d}_k \in \mathbb{C}^{n_d}$ where $n_d \leq N_d$. Here, N_d denotes some system constraint with $1 \leq N_d \leq N_t$ (e.g., the number of available RF chains in the case of hybrid precoding in Section III-B).

In a hybrid beamforming scenario, our goal is to design the pre-beamforming matrix \mathbf{F} that supports a spatial matched filter transmit beamforming (e.g., $\mathbf{v}_k = \hat{\mathbf{h}}_{\ell|\ell} / \|\hat{\mathbf{h}}_{\ell|\ell}\|_2$)² by using channel statistics and training signal design. Here, the pre-beamforming matrix \mathbf{F} is optimized offline and the post-beamforming \mathbf{d}_k is determined with respect to (w.r.t.) transmit beamforming schemes by using the current channel estimate.

²The results can be straightforwardly generalized for any linear transmit beamformings.

A. Review of Prior Work and Motivation for Proposed Scheme

We briefly review other work on the sequential design of the pilot beam pattern for channel estimation in massive MIMO systems. The channel mean square error (MSE) $\text{tr}(\mathbf{P}_{\ell|\ell})$ in (7) depends on the current training signal \mathbf{S}_ℓ and the prediction error covariance $\mathbf{P}_{\ell|\ell-1}$ that is a function of all previous training signals $\mathbf{S}_{\ell-1}$ and the channel statistics (a, \mathbf{R}_h) by the Kalman recursion in (7) and (8). Thus, given the previous training signal $\mathbf{S}_{\ell-1}$, the channel MSE can be minimized by properly designing the pilot beam pattern \mathbf{S}_ℓ . The following proposition presents a property of pilot beam pattern.

Proposition 1: [9] Given all previous pilot signals $\mathbf{S}_{\ell'}$ ($\ell' < \ell$), the pilot beam signal \mathbf{S}_ℓ at the ℓ -th training period minimizing $\text{tr}(\mathbf{P}_{\ell|\ell})$ is given by a properly scaled version of the M_p dominant eigenvectors of the Kalman prediction error covariance matrix $\mathbf{P}_{\ell|\ell-1}$ for the ℓ -th training period.

Proposition 1 states that the use of the M_p dominant eigenvectors of $\mathbf{P}_{\ell|\ell-1}$ for training signals minimizes the channel MSE at the ℓ -th training phase. Under this pilot beam pattern design, all the Kalman matrices $(\mathbf{P}_{\ell|\ell}, \mathbf{P}_{\ell|\ell-1})$ and the channel spatial covariance \mathbf{R}_h are *simultaneously diagonalizable*, i.e., given the ED of \mathbf{R}_h in (3), we have $\mathbf{P}_{\ell|\ell} = \mathbf{U} \bar{\Lambda}^{(\ell)} \mathbf{U}^H$ and $\mathbf{P}_{\ell|\ell-1} = \mathbf{U} \Lambda^{(\ell)} \mathbf{U}^H$ where $\bar{\Lambda}^{(\ell)}$ and $\Lambda^{(\ell)}$ denote diagonal matrices composed of the eigenvalues of $\mathbf{P}_{\ell|\ell}$ and $\mathbf{P}_{\ell|\ell-1}$, respectively. This yields that all the eigenvectors of $\mathbf{P}_{\ell|\ell-1}$ over time are selected from the set of eigenvectors of \mathbf{R}_h defined by $\{\mathbf{u}_1, \dots, \mathbf{u}_r\}$ in (3). However, the pilot beam patterns considered in this approach are inherently obtained in high-dimensional space and also makes a closed-form performance analysis intractable by greedy sequential search of the dominant eigenvectors of $\mathbf{P}_{\ell|\ell-1}$.

Because of the optimal training signals' properties mentioned in Proposition 1, we assume that each training matrix \mathbf{S}_ℓ is a scaled version of M_p eigenvectors of \mathbf{R}_h in (3) to satisfy the power constraint. From (6), the channel estimate at the ℓ -training period is a *linear* combination of all previously used training signals $\mathbf{S}_\ell := \{\mathbf{S}_{\ell'} : \ell' \leq \ell\}$ by Kalman recursion in (7) and (8), i.e., the channel estimate $\hat{\mathbf{h}}_{\ell|\ell}$ lies in the column space of \mathbf{S}_ℓ . That is, in the hybrid beamforming structure of $\mathbf{v}_k = \mathbf{F} \mathbf{d}_k$, we require that the pre-beamforming matrix \mathbf{F} spans the subspace spanned by the training signal \mathbf{S}_ℓ for subspace sampling of the channel estimate. Therefore, the training signal \mathbf{S}_ℓ should be suitably designed to capture the n_d dominant channel eigenmodes under the $n_d \leq N_d$ dimensionality constraint where the variable n_d should be properly optimized to account for the effective channel rank. Note that the pre-beamforming matrix \mathbf{F} is then determined by a set of n_d distinct eigenvectors of \mathbf{R}_h used in the training signals \mathbf{S}_ℓ .

Alternatively, based on the Toeplitz distribution theorem to large-scale linear antenna arrays, the eigenvectors of the correlation matrix \mathbf{R}_h are well approximated by columns of

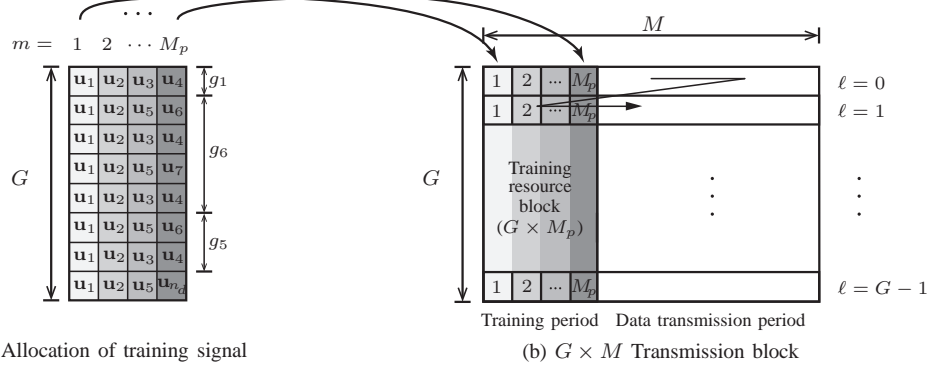


Fig. 2. A training frame composed of G consecutive block transmissions where $G = 8$, $M_p = 4$, $n_d = 8$, and symbol time $k = \ell M + m$

a unitary *discrete Fourier transform* (DFT) matrix. Then, the pre-beamformer can be designed using some columns of the DFT matrix used in the training signals, as later discussed in Section III-B.

We can write each $\mathbf{S}_\ell \in \mathbb{C}^{N_t \times M_p}$ as a $1 \times M_p$ vector where the i -th entry of the vector equals to the index of the eigenvector of \mathbf{R}_h that defines the i -th column of \mathbf{S}_ℓ . For example, if $\mathbf{S}_0 = \sqrt{\rho}[\mathbf{u}_1, \mathbf{u}_2, \mathbf{u}_3, \mathbf{u}_4]$ and $\mathbf{S}_1 = \sqrt{\rho}[\mathbf{u}_1, \mathbf{u}_2, \mathbf{u}_5, \mathbf{u}_6]$ are given for $M_p = 4$, those training signals are characterized by the index vectors of $[1, 2, 3, 4]$ and $[1, 2, 5, 6]$, respectively. By collecting G consecutive training periods to define the training signal $\mathcal{S}_{G-1} = \{\mathbf{S}_\ell : 0 \leq \ell < G\}$, we can then succinctly define the training signal \mathcal{S}_{G-1} by an index matrix $\mathbf{C} \in \mathbb{C}^{G \times M_p}$ with each row representing the eigenvector indices used during the corresponding training period. For example, Fig. 2(b) shows a $G \times M_p$ training resource block where the training signal matrix \mathbf{S}_ℓ will be transmitted at the ℓ -th training period where $0 \leq \ell < G$. An example of the index matrix with $G = 8$ and $M_p = 4$ in Fig. 2 is given by

$$\mathbf{C} = \begin{bmatrix} 1 & 1 & 1 & 1 & 1 & 1 & 1 & 1 \\ 2 & 2 & 2 & 2 & 2 & 2 & 2 & 2 \\ 3 & 5 & 3 & 5 & 3 & 5 & 3 & 5 \\ 4 & 6 & 4 & 7 & 4 & 6 & 4 & 8 \end{bmatrix}^T, \quad (9)$$

then we have the ℓ -th training signal matrix $\mathbf{S}_\ell = \sqrt{\rho}[\mathbf{u}_{[\mathbf{C}]_{\ell+1,1}}, \mathbf{u}_{[\mathbf{C}]_{\ell+1,2}}, \dots, \mathbf{u}_{[\mathbf{C}]_{\ell+1,M_p}}]$ where $0 \leq \ell < G$.

We have discussed how the index matrix \mathbf{C} defines the training signals $\{\mathbf{S}_\ell : 0 \leq \ell < G\}$ where we will refer to \mathbf{C} as the *training sequence* (index) matrix. In the next section, we present a systematic approach to the training sequence optimization.

III. PROPOSED TRAINING SEQUENCE FRAMEWORK

In this section, we first focus on the design of a reduced dimensionality training sequence that has a suitable mapping to training signals used during the training phases. We next provide a hybrid analog-digital beamforming method that exploits the limited number of available RF chains relative to the number of antennas.

A. Training Sequence Design

To construct the training sequence \mathbf{C} , we need to define how the selected n_d eigenvectors will be allocated in the G consecutive training periods. We assume that each of the selected eigenvectors will not be transmitted more than once within each of the training periods in order to allocate the training signals across G training phases. Note that in this case each training signal matrix \mathbf{S}_ℓ is composed of M_p distinct eigenvectors. Therefore, for each ℓ , $\mathbf{S}_\ell^H \mathbf{S}_\ell = \mathbf{I}_{M_p}$. For $1 \leq i \leq n_d$, denote by g_i the block time-wise interval where if \mathbf{u}_i is firstly used as a training signal at symbol time $\tilde{\ell}M + m$ for $0 \leq \tilde{\ell} < G$, $1 \leq m \leq M_p$, and $0 < g_i \leq G$, the training signal on \mathbf{u}_i will be re-transmitted at symbol time $(\tilde{\ell} + g_i \cdot (\ell)_{G/g_i})M + m$ for $0 \leq \ell < G$. Here, $(\cdot)_b$ denotes the integer modulo b . For $n_d < i \leq N_t$, we set $g_i = 0$ because \mathbf{u}_i is not used as a training signal. An example with $g_1 = g_2 = 1$, $g_3 = g_4 = g_5 = 2$, $g_6 = 4$, $g_7 = g_8 = 8$, and $n_d = 8$ is shown in Fig. 2(a).

The dimension of the offline-designed precoder n_d is clearly constrained by the system. First, the training signal construction allows the transmitter to sound *at least* M_p different subspace dimensions. Therefore, n_d should be restricted to be at least M_p in order to span as large of a subspace as possible. In the same way, the transmitter structure (e.g., hybrid precoder structure) means that the precoder must satisfy $n_d \leq N_d$ and $n_d \leq r$ where $\text{rank}(\mathbf{R}_h) = r$ in (3). Second, a training frame can sound *at most* GM_p different dimensions. Thus, $n_d \leq GM_p$. Therefore, we notice that the number of distinct eigenvectors (n_d) used in the training sequence should satisfy $M_p \leq n_d \leq \min\{GM_p, N_d, r\}$. The unknown parameter n_d should be jointly optimized with $\{g_i\}$, which defines the training sequence \mathbf{C} . We then consider the following condition for the design of training sequence.

(C.1) For each i ($1 \leq i \leq n_d$), the block time-wise interval g_i is a divisor of G , i.e., $g_i \in \mathcal{I}_G := \{d_j | (G)_{d_j} = 0 \text{ for } 1 \leq d_j \leq G \text{ and } d_j < d_{j+1}\}$, then we have an integer of G/g_i .

Condition (C.1) guarantees that once the training sequence $\mathbf{C} \in \mathbb{N}^{G \times M_p}$ is designed with n_d and $\{g_i\}$, the training sequence can be used for all subsequent training frames due to the periodic pilot allocation patterns, i.e., we transmit the

training signals $\mathbf{S}_\ell = \mathbf{S}_{(\ell)_G}$ where $\ell = 0, 1, \dots$. Note that, when $G = 2^s$ for some nonnegative integer s , the set of divisors of G is given by

$$\mathcal{I}_G = \{1, 2, \dots, 2^{s-1}, 2^s\}. \quad (10)$$

Given the block time-wise vector $\mathbf{g} = [g_1, g_2, \dots, g_{n_d}]^T$ satisfying (C.1), the training signal vectors $\{\mathbf{u}_i : 1 \leq i \leq n_d\}$ are interspersed corresponding to the block time-wise intervals $\{g_i\}$ across G consecutive training phases. Thus, when the training signal of \mathbf{u}_i is not used during $g_i - 1$ inter-block symbol times, the channel MSE along the direction of \mathbf{u}_i monotonically increases by (8) where $1 \leq i \leq n_d$. Given this, we evaluate the channel estimation performance by deriving the minimum steady-state channel MSE for $1 \leq i \leq n_d$ given by

$$\lambda_{i,g_i}^{(\infty)} := \lim_{\ell \rightarrow \infty} \bar{\lambda}_i^{(\ell)} \quad (11)$$

$$\begin{aligned} &= \frac{(a^{2g_i} \lambda_{i,g_i}^{(\infty)} + (1 - a^{2g_i}) \lambda_i)}{\rho(a^{2g_i} \lambda_{i,g_i}^{(\infty)} + (1 - a^{2g_i}) \lambda_i) + 1} \\ &= \frac{\lambda_i}{\left(\frac{1}{2}(1 + \lambda_i \rho)\right) + \sqrt{\left(\frac{1}{2}(1 + \lambda_i \rho)\right)^2 + \frac{a^{2g_i}}{1 - a^{2g_i}} \lambda_i \rho}}, \end{aligned} \quad (12)$$

from the Riccati equation [18]

$$\bar{\lambda}_i^{(\ell)} = \frac{(a^{2g_i} \bar{\lambda}_i^{(\ell-g_i)} + (1 - a^{2g_i}) \lambda_i)}{\rho(a^{2g_i} \bar{\lambda}_i^{(\ell-g_i)} + (1 - a^{2g_i}) \lambda_i) + 1}, \quad (14)$$

where $\bar{\boldsymbol{\lambda}}^{(\ell)} = [\bar{\lambda}_1^{(\ell)}, \dots, \bar{\lambda}_r^{(\ell)}]^T := \text{diag}(\bar{\boldsymbol{\Lambda}}^{(\ell)})$ and $\boldsymbol{\lambda} = [\lambda_1, \dots, \lambda_r]^T := \text{diag}(\boldsymbol{\Lambda})$ denote the eigenvalues of $\mathbf{P}_{\ell|\ell}$ and \mathbf{R}_h , respectively. Here, the minimum steady-state channel MSE of $\lambda_{i,g_i}^{(\infty)}$ is obtained when the training signal corresponding to \mathbf{u}_i is transmitted according to the block time-wise interval g_i at training phases.

Once the training signal corresponding to \mathbf{u}_i is transmitted, the training signal is not transmitted during the next $g_i - 1$ successive blocks. During these blocks, the minimum steady-state channel MSE $\lambda_{i,g_i}^{(\infty)}$ grows up by (8) because the Kalman filter predicts the channel state along the direction of the training signal. In this case, the maximum steady-state MSE of the training signal (denoted as $\lambda_{i,g_i}^{(\infty)}$) is reached after the $g_i - 1$ transmission blocks and is given by

$$\lambda_{i,g_i}^{(\infty)} := a^{2(g_i-1)} \lambda_{i,g_i}^{(\infty)} + (1 - a^{2(g_i-1)}) \lambda_i, \quad (15)$$

where $1 \leq i \leq n_d$. Note that the steady-state channel MSEs of the unused eigenvectors in the training sequence remain constant over time, i.e., $\lim_{\ell \rightarrow \infty} \lambda_i^{(\ell)} = \lambda_i$ for $n_d < i \leq r$.

Remark 1: From (13) and (15), the steady-state channel MSE is bounded by

$$\text{diag}(\boldsymbol{\lambda}_g^{(\infty)}) \preceq \lim_{\ell \rightarrow \infty} \mathbf{P}_{\ell|\ell} \preceq \text{diag}(\boldsymbol{\lambda}_g^{(\infty)}), \quad (16)$$

where $\boldsymbol{\lambda}_g^{(\infty)} = [\lambda_{1,g_1}^{(\infty)}, \dots, \lambda_{n_d,g_{n_d}}^{(\infty)}, \lambda_{n_d+1}, \dots, \lambda_r]^T$ and $\boldsymbol{\lambda}_g^{(\infty)}$ is similarly defined. $\mathbf{A} \succeq 0$ denotes a positive semidefinite matrix. The gap between upper and lower

bounds for the steady-state channel MSE $\text{tr}(\mathbf{P}_{\ell|\ell})$ is given by $\sum_{i=1}^{n_d} (1 - a^{2(g_i-1)}) (\lambda_i - \lambda_{i,g_i}^{(\infty)})$.

Note that the trace of the steady-state channel MSE is bounded by $\|\boldsymbol{\lambda}_g^{(\infty)}\|_1$ in (16), then we formulate the optimization problem that designs the training sequence by minimizing an upper bound on the steady-state channel MSE, which is formally stated as follows.

Problem 1: Given the parameters (G, M_p, N_d, r) , the optimal \mathbf{g}^* and n_d^* are chosen as the minimizers of

$$\min_{\mathbf{g}, n_d} \|\boldsymbol{\lambda}_g^{(\infty)}\|_1 \quad (17)$$

subject to (C.1) and $M_p \leq n_d \leq \min\{GM_p, N_d, r\}$

$$\sum_{i=1}^{n_d} \frac{1}{g_i} = M_p. \quad (18)$$

The nonlinear constraint (18) yields a total training resource constraint in the $G \times M_p$ training sequence. That is, for $1 \leq i \leq n_d$, each training signal \mathbf{u}_i is transmitted according to the block time-wise interval g_i across the G consecutive training phases where the training signal on \mathbf{u}_i is transmitted G/g_i times during the training phases. Then the total number of transmission blocks for the n_d training signals should be equal to GM_p , i.e., $\sum_{i=1}^{n_d} G/g_i = GM_p$. The nonlinear inequality (18) and the periodicity condition of (C.1) make solving Problem 1 extremely difficult, particularly because the optimization variables \mathbf{g} and n_d are interconnected.

To tackle the challenge of this problem, we first consider exhaustive search in a finite search space that arises from the integer constraint of Problem 1. In this case, it is important to reduce the computational complexity of the exhaustive search, and thus we derive a property of the objective function in (17).

Proposition 2: $\lambda_{i,g_i}^{(\infty)}$ is a monotonic increasing function of g_i , i.e., $\lambda_{i,g'_i}^{(\infty)} \leq \lambda_{i,g_i}^{(\infty)}$ if $1 \leq g'_i \leq g_i$.

Proof: See Appendix A.

Proposition 2 shows that the maximum steady-state channel MSE of $\lambda_{i,g_i}^{(\infty)}$ is monotonically reduced with decreasing g_i (i.e., MSE is reduced by transmitting the training signal corresponding to \mathbf{u}_i more frequently). Thus, we assume that the block time-wise interval \mathbf{g} is arranged in ascending order such that $g_i \leq g_j$ for $i \leq j$ in order to effectively minimize the dominant channel MSE of $\boldsymbol{\lambda}_g^{(\infty)}$ that corresponds to the dominant channel directions. It is numerically confirmed that the assumption of the ordered \mathbf{g} is consistent with the result of the exhaustive search and yields a much simpler implementation compared to the initial number of trials for the exhaustive search $\mathcal{O}(|\mathcal{I}_G|^{\min\{GM_p, N_d, r\}})$. Furthermore, by exploiting the monotonicity in Proposition 2, we propose an efficient algorithm for training sequence design that sequentially minimizes the maximum upper bound of the steady-state channel MSE. The corresponding algorithm is summarized in Algorithm 1, which requires substantially

less computational complexity $\mathcal{O}(GM_p)$ while achieving most of the performance gain compared to the exhaustive search. Simulation results will be provided in Section V.

Algorithm 1 Min-Max Training Sequence Design

Require: Perform the ED of $\mathbf{R}_h = \mathbf{U}\mathbf{\Lambda}\mathbf{U}^H$. Store $\boldsymbol{\lambda} = \text{diag}(\mathbf{\Lambda})$.

Set $\mathbf{g} = (G+1)\mathbf{1}_{N_t \times 1}$, $\mathbf{q} = \mathbf{0}_{N_t \times 1}$, $\boldsymbol{\lambda}_g^{(\infty)} = \boldsymbol{\lambda}$, $\mathcal{N}_d = \{1, \dots, N_d\}$, and $N_{blk} = GM_p$.

while $N_{blk} > 0$ **do**

$$\begin{cases} i' = \arg\max_{i \in \mathcal{N}_d} \lambda_{i,g_i}^{(\infty)} \\ d^* = \max_{j: d_j < g_{i'}} d_j \text{ where } d_j \in \mathcal{I}_G \end{cases} \quad (\text{Step } \dagger)$$

if $(N_{blk} + q_{i'} \cdot G/g_{i'}) \geq G/d^*$ **then**

$$N_{blk} \leftarrow (N_{blk} + q_{i'} \cdot G/g_{i'}) - G/d^*$$

$$g_{i'} \leftarrow d^*$$

$$q_{i'} = 1$$

$$\lambda_{i',g_{i'}}^{(\infty)} = a^{2(g_{i'}-1)} \lambda_{i',g_{i'}}^{(\infty)} + (1 - a^{2(g_{i'}-1)}) \lambda_{i'}$$

else

$$\mathcal{N}_d \leftarrow \mathcal{N}_d \setminus \{i'\}$$

end if

end while

$$\mathbf{g} = \mathbf{g}(\mathbf{q}) \quad (\text{Step } \ddagger)$$

(Here, Step \dagger is to sequentially minimize the maximum steady-state channel MSE by reducing the interval g_i and Step \ddagger is to select some entries of \mathbf{g} optimized in this algorithm.)

Since the design of the block time-wise interval \mathbf{g} and n_d is complete, we finish this subsection by explaining the construction of \mathbf{C} from the optimized intervals $\{g_i : g_i = 2^{k_i} \in \mathcal{I}_G \text{ in (10), } 1 \leq i \leq n_d\}$ which uses the assumption that $G = 2^s$. Note that, given a set of $\{g_1, \dots, g_{n_d}\}$, there can be several (row-wise and column-wise) permuted versions of a training signal allocation in the training sequence \mathbf{C} . However, they have the same steady-state performance, with only minor changes during the transient phase. Thus, we present an efficient method for construction of \mathbf{C} which is done iteratively.

A new variable U_j represents the number of undetermined entries of the j -th column of the matrix \mathbf{C} , which is initially set to $U_j = G$ for $1 \leq j \leq M_p$. Denote by q the row index of the matrix \mathbf{C} for $1 \leq q \leq G$. First, we set the initial values as $q = 1$, and $I_q = 1$, and then we loop over all row indices q in order to determine the entries of \mathbf{C} as follows.

Step (1) Given q , I_q , and U_j , select a column index $j' \in \{1, \dots, M_p\}$ of \mathbf{C} such that $[\mathbf{C}]_{q,j'}$ is not determined while $\{[\mathbf{C}]_{q,1}, \dots, [\mathbf{C}]_{q,j'-1}\}$ are all determined by some eigenvector indices in the previous step (e.g., $j' = 1$ at the first iteration). We then allocate the eigenvector index of $i_{q,j} := I_q + (j - j')$ at the j -th column with a row-wise mapping $g_{i_{q,j}}$. Mathematically, this means

$$[\mathbf{C}]_{q,j} = [\mathbf{C}]_{g_{i_{q,j}}+q,j} = \dots = [\mathbf{C}]_{(G/g_{i_{q,j}}-1)g_{i_{q,j}}+q,j} = i_{q,j}, \quad (19)$$

where $j' \leq j \leq M_p$. Note that $G/g_{i_{q,j}}$ entries of the j -th column are determined using a row-wise allocation of $i_{q,j}$

while leaving its $U_j - G/g_{i_{q,j}}$ undetermined entries.³ For the next step, we update the variables given by

$$\begin{aligned} I_{q+1} &= I_q + M_p - j' + 1, & U_j &= U_j - G/g_{i_{q,j}}, \text{ and} \\ q &= q + 1. \end{aligned} \quad (20)$$

Step (2) Repeat *Step (1)* until all entries of \mathbf{C} are determined, i.e., $U_j = 0$ for all j .

Corollary 1: Given the constraints of Problem 1 and the arranged block time-wise interval \mathbf{g} in ascending order, if $G = p^s$ for some prime number p and nonnegative number s , a training sequence \mathbf{C} can be constructed.

Proof: See Appendix B.

B. Hybrid Analog-Digital Precoding

We assume that the antenna arrays are uniformly placed in a 1-dimensional or 2-dimensional space at the base station, where the channel covariance matrix \mathbf{R}_h becomes Toeplitz under a far-field assumption. It is known that when the size of a Toeplitz matrix is large, the Toeplitz matrix can be decomposed by a DFT matrix, referred to as the Toeplitz distribution theorem (TDT) [19], [20], i.e.,

$$\mathbf{R}_h = E\{\mathbf{h}_\ell \mathbf{h}_\ell^H\} = \tilde{\mathbf{F}} \mathbf{\Lambda} \tilde{\mathbf{F}}^H, \quad (21)$$

where $\tilde{\mathbf{F}} = [\tilde{\mathbf{f}}_1, \dots, \tilde{\mathbf{f}}_r] \in \mathbb{C}^{N_t \times r}$ denotes a matrix of distinct columns of the N_t -point DFT matrix and $\mathbf{\Lambda} = \text{diag}(\lambda_1, \dots, \lambda_r)$ is a matrix of the non-zero eigenvalues of \mathbf{R}_h in descending order. Note that the k -th column of $\tilde{\mathbf{F}}$ is given by

$$\frac{1}{\sqrt{N_t}} [1, e^{j1\psi_k 2\pi/N_t}, e^{j2\psi_k 2\pi/N_t}, \dots, e^{j(N_t-1)\psi_k 2\pi/N_t}]^H.$$

This is simply the transmit steering vector for the physical angle $\theta_k = \sin^{-1}(\psi_k \lambda/d)$,⁴ and thus the diagonal matrix $\mathbf{\Lambda}$ can be viewed as the channel power spectral density corresponding to the virtual angular domain.

In this case, the channel dynamics in (2) is rewritten by a parametric channel model [21], [22]

$$\mathbf{h}_{\ell+1} = a\mathbf{h}_\ell + \sqrt{1-a^2} \tilde{\mathbf{F}} \mathbf{\Lambda}^{1/2} \tilde{\mathbf{b}}_{\ell+1}, \quad (22)$$

where the entries of $\tilde{\mathbf{b}}_\ell$ are independent and identically distributed (i.i.d.), i.e., $\tilde{\mathbf{b}}_\ell \sim \mathcal{CN}(\mathbf{0}, \mathbf{I}_r)$. This yields that the channel vector is characterized by a random linear combination of the columns of $\tilde{\mathbf{F}}$ and channel estimation can be viewed as estimation of the linear combination coefficients corresponding to the set of bases vectors $\tilde{\mathbf{F}}$. Thus, we use the DFT-based training signal (i.e., $\mathbf{S}_\ell \subset \{\tilde{\mathbf{f}}_i\}$) during the training phase because the columns of DFT are approximated eigenvectors of the channel spatial correlation \mathbf{R}_h in (21).

³If all elements of the q -th row of \mathbf{C} are determined, we complete *Step (1)* by updating $I_{q+1} = I_q$ and $q = q + 1$ with the same U_j .

⁴The virtual angle ψ_k is related to the physical angle θ_k by $\psi = \frac{d}{\lambda} \sin(\theta_k)$, i.e., if $d/\lambda = 1/2$, $-\frac{\pi}{2} \leq \theta_k \leq \frac{\pi}{2}$ corresponds to $-\frac{1}{2} \leq \psi_k \leq \frac{1}{2}$, where d and λ denote the antenna spacing and the carrier wavelength, respectively [9].

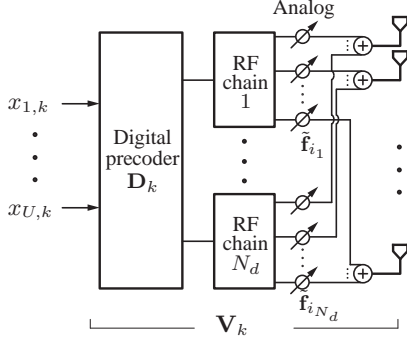


Fig. 3. Hybrid beamforming architecture with digital precoding $\mathbf{D}_k \in \mathbb{C}^{n_d \times U}$ and analog precoding $\{\hat{\mathbf{f}}_i\}$ for U data streams ($U \leq n_d \leq N_d$)

During the ℓ -th data transmission phase (i.e., $k = \ell M + m$ and $M_p < m \leq M$), we assume that the data symbol sequence $\{x_{u,k}\}$ is transmitted with the multi-dimensional transmit beamformer $\mathbf{V}_k \in \mathbb{C}^{N_t \times U}$, as shown in Fig. 3. Here, we assume that the base station is equipped with $1 \leq N_d \leq N_t$ available RF chains for digital baseband precoding of $\mathbf{D}_k \in \mathbb{C}^{n_d \times U}$, given by $\mathbf{V}_k = \mathbf{F}\mathbf{D}_k$ where a pre-beamforming matrix $\mathbf{F} \in \mathbb{C}^{N_t \times n_d}$ is implemented by analog beamforming techniques (e.g., use analog phase shifters with constant magnitude entries). Here, the variable $n_d \leq N_d$ denotes the number of used RF chains to have a low-dimensional solution while capturing the effective channel rank aimed at enabling low-complexity and energy-efficient system implementation.

As explained in Section II, the ℓ -th channel estimate $\hat{\mathbf{h}}_{\ell|\ell}$ lies in the column space of all the used training signal \mathcal{S}_ℓ composed of the DFT columns. Then, the pre-beamforming \mathbf{F} will span the subspace of the training signal \mathcal{S}_ℓ , i.e., the pre-beamforming matrix is determined by the distinct DFT columns used in the construction of the training sequence that specifies the training signals. Therefore, we focus on the design of the DFT-based training sequence under the constraint of the N_d available RF chains. To meet the constraint on the RF chains, we restrict the number of distinct DFT columns (n_d) used in the training sequence to be less than or equal to N_d . Such a design is obtained from the proposed methods of Problem 1 by substituting the eigenvalues $\mathbf{\Lambda}$ of (21) into (13) and (15). Simulations will be presented in Section V where the training signals are approximated by DFT vectors without much loss in performance.

IV. EXTENSION TO MULTI-USER MASSIVE MIMO

A. System Set-Up

Consider the downlink of a cellular system serving U single antenna users. Let $\mathbf{h}_{u,\ell} \in \mathbb{C}^{N_t}$ be the channel vector of user u at the ℓ -th block symbol time where $1 \leq u \leq U$. In line with (2), we consider a state-space model for $\mathbf{h}_{u,\ell}$ with the channel covariance matrix $\mathbf{R}_{\mathbf{h}_u} = E\{\mathbf{h}_{u,\ell}\mathbf{h}_{u,\ell}^H\}$ such that $\text{rank}(\mathbf{R}_{\mathbf{h}_u}) = r_u$. Define $\mathbf{H}_\ell = [\mathbf{h}_{1,\ell}, \dots, \mathbf{h}_{U,\ell}] \in \mathbb{C}^{N_t \times U}$ as the combined channel matrix for a block length of M channel uses. Denote by $\mathbf{x}_k = [x_{1,k}, \dots, x_{U,k}]^T \in \mathbb{C}^U$

be the data symbols at the symbol time $k = \ell M + m$ to service U user terminals with the same average transmit power of ρ so that $E\{|x_{u,k}|^2\} = \rho$. We assume that the base station uses the multi-dimensional transmit beamformer $\mathbf{V}_k = [\mathbf{v}_{1,k}, \dots, \mathbf{v}_{U,k}] \in \mathbb{C}^{N_t \times U}$ to map \mathbf{x}_k to the transmit antennas, i.e., $\mathbf{s}_k = \mathbf{V}_k \mathbf{x}_k$. Denote by $n_{d,u}$ the number of disjoint training signals used in the construction of the training sequence to service the user u .

The collection of received symbols for all U users at the ℓ -th data transmission period (i.e., channels uses satisfying $k = \ell M + m$ with $M_p < m \leq M$) is denoted as

$$\mathbf{y}_k = \sqrt{\alpha} \mathbf{H}_\ell^H \mathbf{V}_k \mathbf{x}_k + \mathbf{w}_k \quad (23)$$

$$= \sqrt{\alpha} \begin{bmatrix} \mathbf{h}_{1,\ell}^H \mathbf{v}_{1,k} & \mathbf{h}_{1,\ell}^H \mathbf{v}_{2,k} & \dots & \mathbf{h}_{1,\ell}^H \mathbf{v}_{U,k} \\ \mathbf{h}_{2,\ell}^H \mathbf{v}_{1,k} & \mathbf{h}_{2,\ell}^H \mathbf{v}_{2,k} & \dots & \mathbf{h}_{2,\ell}^H \mathbf{v}_{U,k} \\ \vdots & \vdots & \ddots & \vdots \\ \mathbf{h}_{U,\ell}^H \mathbf{v}_{1,k} & \mathbf{h}_{U,\ell}^H \mathbf{v}_{2,k} & \dots & \mathbf{h}_{U,\ell}^H \mathbf{v}_{U,k} \end{bmatrix} \mathbf{x}_k + \mathbf{w}_k,$$

where $\mathbf{y}_k = [y_{1,k}, \dots, y_{U,k}]^T$ and $\mathbf{w}_k \sim \mathcal{CN}(0, \mathbf{I}_U)$ is the additive white Gaussian noise vector, and α is the power normalization to satisfy the average transmit power constraint so that $\alpha = 1/E\{\text{tr}(\mathbf{V}_k^H \mathbf{V}_k)\}$. Focusing only on the received signal for user u , we have

$$y_{u,k} = \sqrt{\alpha} \mathbf{h}_{u,\ell}^H \mathbf{v}_{u,k} x_{u,k} + \sqrt{\alpha} \sum_{u' \neq u} \mathbf{h}_{u,\ell}^H \mathbf{v}_{u',k} x_{u',k} + w_{u,k}$$

$$\stackrel{(a)}{=} \sqrt{\alpha} \mathbf{h}_{u,\ell}^H \hat{\mathbf{h}}_{u,\ell|\ell} x_{u,k} + \sqrt{\alpha} \sum_{u' \neq u} \mathbf{h}_{u,\ell}^H \hat{\mathbf{h}}_{u',\ell|\ell} x_{u',k} + w_{u,k}$$

$$\stackrel{(b)}{=} \sqrt{\alpha} \hat{\mathbf{h}}_{u,\ell|\ell}^H \hat{\mathbf{h}}_{u,\ell|\ell} x_{u,k} + \sqrt{\alpha} \tilde{\mathbf{h}}_{u,\ell}^H \hat{\mathbf{h}}_{u,\ell|\ell} x_{u,k}$$

$$+ \sqrt{\alpha} \sum_{u' \neq u} \mathbf{h}_{u,\ell}^H \hat{\mathbf{h}}_{u',\ell|\ell} x_{u',k} + w_{u,k}, \quad (24)$$

where (a) follows the matched filtering precoder $\mathbf{v}_{u,k} = \hat{\mathbf{h}}_{u,\ell|\ell}$ and (b) holds by $\tilde{\mathbf{h}}_{u,\ell} := \mathbf{h}_{u,\ell} - \hat{\mathbf{h}}_{u,\ell|\ell}$.

Applying the method in [23], a lower bound on the training-based capacity is obtained by considering the worst-case uncorrelated additive noise. From (24), we have the SINR of user u as

$$\text{SINR}_{u,\ell} := \frac{\eta_{u,\ell}}{\sigma_{u,\ell}^2}, \quad (25)$$

where the desired signal power (scaled by $\frac{1}{\alpha\rho}$) is given by

$$\eta_{u,\ell} = |\hat{\mathbf{h}}_{u,\ell|\ell}^H \hat{\mathbf{h}}_{u,\ell|\ell}|^2,$$

and the interference plus noise power is given by

$$\sigma_{u,\ell}^2 = \frac{1}{\alpha\rho} + |\tilde{\mathbf{h}}_{u,\ell}^H \hat{\mathbf{h}}_{u,\ell|\ell}|^2 + \sum_{u'=1:u' \neq u} |\mathbf{h}_{u,\ell}^H \hat{\mathbf{h}}_{u',\ell|\ell}|^2.$$

B. Performance Analysis

In order to find a convenient expression for the SINR in (25), we focus on the asymptotic results when $N_t \rightarrow \infty$ in [6]. For simplicity, we assume a symmetric scenario with the same number $n_{d,u} = n_d$ for users. The results proposed here, however, extends immediately to the general case. The

following proposition provides a closed-form expression of the SINR.

Proposition 3: The deterministic equivalent SINR of (25) under a Kalman filtering framework is given by

$$\overline{\text{SINR}}_{u,\ell} \stackrel{N_t \rightarrow \infty}{=} \frac{A_{u,\ell}}{\frac{1}{\alpha\rho} + B_{u,\ell} + C_{u,\ell}}, \quad (26)$$

where

$$A_{u,\ell} = |\text{tr}(\mathbf{\Lambda}_u - \bar{\mathbf{\Lambda}}_u^{(\ell)})|^2 \quad (27)$$

$$B_{u,\ell} = \text{tr}(\bar{\mathbf{\Lambda}}_u^{(\ell)} (\mathbf{\Lambda}_u - \bar{\mathbf{\Lambda}}_u^{(\ell)})) \quad (28)$$

$$C_{u,\ell} = \sum_{u'=1:u' \neq u}^U \text{tr}(\mathbf{\Lambda}_u \mathbf{U}_u^H \mathbf{U}_{u'} (\mathbf{\Lambda}_{u'} - \bar{\mathbf{\Lambda}}_{u'}^{(\ell)}) \mathbf{U}_{u'}^H \mathbf{U}_u). \quad (29)$$

Given the ED of $\mathbf{R}_{\mathbf{h}_u} = \mathbf{U}_u \mathbf{\Lambda}_u \mathbf{U}_u^H$ where $\mathbf{U}_u \in \mathbb{C}^{N_t \times r_u}$ and $\mathbf{\Lambda}_u = \text{diag}(\lambda_{u,1}, \dots, \lambda_{u,r_u})$ composed of the non-zero eigenvalues in descending order, the estimation error covariance matrix $\mathbf{P}_{u,\ell|\ell}$ is eigen-decomposed by $\mathbf{P}_{u,\ell|\ell} = \mathbf{U}_u \bar{\mathbf{\Lambda}}_u^{(\ell)} \mathbf{U}_u^H$.

Proof: See Appendix C.

The three terms in the denominator of (26) characterize the following effects: $1/(\alpha\rho)$ for the post-processed (average) transmit signal-to-noise power ratio, $B_{u,\ell}$ for imperfect channel estimation, and $C_{u,\ell}$ for inter-user interference from the other users sharing the same time-frequency slot. Proposition 3 provides some intuition about how the SINR can be analyzed in training-based channel estimation. First, in order to maximize $A_{u,\ell}$ of (27), the diagonal entries of $\bar{\mathbf{\Lambda}}_u^{(\ell)}$ should be minimized according to the absolute values of the diagonal entries of $\mathbf{\Lambda}_u$. Note that the proposed training sequence design can be leveraged to increase $A_{u,\ell}$ because the training sequence \mathbf{C} reduces the n_d^* dominant eigenvalues of $\bar{\mathbf{\Lambda}}_u^{(\ell)}$ by using its n_d^* dominant eigenvectors of $\mathbf{R}_{\mathbf{h}_u}$ as training signals corresponding to the block time-wise interval \mathbf{g}^* . Here, \mathbf{g}^* and n_d^* denote the minimizers of Problem 1 obtained by the proposed algorithm. On the one hand, $B_{u,\ell}$ of (28) can be viewed as a weighed version of $A_{u,\ell}$ where we can constrain $B_{u,\ell}$ through the training sequence design by reducing the dominant entries of $\bar{\mathbf{\Lambda}}_u^{(\ell)}$. Second, $C_{u,\ell}$ of (29) can be reduced when the users serviced simultaneously on the same time-frequency are scheduled so that the dominant eigenvectors of the users are orthogonal to each other. Here, user scheduling techniques can be applied w.r.t. the angle-of-arrival range and angle spread [13], [14].⁵

For performance metric analysis, the expression of (48) can be precomputed before the Kalman filter is run and the (deterministic) achievable throughput for user u at the ℓ -th

block is given by [6]

$$R_{u,\ell} = \left(1 - \frac{M_p}{M}\right) \cdot \log(1 + \overline{\text{SINR}}_{u,\ell}), \quad (30)$$

where the pre-log factor $(1 - M_p/M)$ is needed because M_p out of over M channel uses is allocated for training.

Based on the closed-form expressions for the steady-state channel MSE in (13) and (15), we further derive a closed-form lower bound of (26), given by

$$\begin{aligned} \overline{\text{SINR}}_u &= \lim_{\ell \rightarrow \infty} \overline{\text{SINR}}_{u,\ell} \\ &\geq \|\boldsymbol{\lambda}_u - \boldsymbol{\lambda}_{\mathbf{g}_u}^{(\infty)}\|_1^2 \left(\frac{1}{\alpha\rho} + \|\boldsymbol{\lambda}_{\mathbf{g}_u}^{(\infty)} \odot (\boldsymbol{\lambda}_u - \boldsymbol{\lambda}_{\mathbf{g}_u}^{(\infty)})\|_1 \right. \\ &\quad \left. + \sum_{u' \neq u} \text{tr}(\mathbf{\Lambda}_u \mathbf{U}_u^H \mathbf{U}_{u'} (\mathbf{\Lambda}_{u'} - \boldsymbol{\Lambda}_{\mathbf{g}_{u'}}^{(\infty)}) \mathbf{U}_{u'}^H \mathbf{U}_u) \right)^{-1}. \end{aligned} \quad (31)$$

A complete derivation of (31) is available in Appendix D.

V. NUMERICAL RESULTS

In this section, we provide numerical results to evaluate the performance of the proposed algorithms. We considered $N_t \in \{128, 375\}$ transmit ULA to serve multiple single antenna users. For the time-varying channel model in (2), we adopted $f_c = 2.5 \text{ GHz}$ carrier frequency and $T_s = 0.5 \text{ ms}$ symbol duration with a typical mobile speed range from $v = 3 \text{ km/h}$ ($a = 0.9999$) to 30 km/h ($a = 0.9881$).⁶ We consider channel estimation performance using the normalized mean square error (NMSE), given by $\text{NMSE} = \text{tr}(\mathbf{P}_{\ell|\ell})/\text{tr}(\mathbf{R}_{\mathbf{h}})$. The channel estimation performance for each of the considered methods was averaged over 500 Monte Carlo runs.

To generate a realistic channel for simulation, we adopt the *one-ring* channel model that well models typical cellular systems [12], [24]. The channel spatial correlation is characterized by angle spread (AS: Δ), angle-of-arrival (AoA: θ), and antenna geometry. Based on the one-ring channel model, we considered a 15×25 uniform planar array at the base station. Then, the channel covariance matrix $\mathbf{R}_{\mathbf{h}}$ is given by $\mathbf{R}_{\mathbf{h}} = \mathbf{R}_H \otimes \mathbf{R}_V$ where $\mathbf{R}_H \in \mathbb{C}^{N_H \times N_H}$ and $\mathbf{R}_V \in \mathbb{C}^{N_V \times N_V}$ denote the horizontal and vertical covariance matrices, respectively, where each of the spatial correlation matrices is defined by

$$[\mathbf{R}_t]_{p,q} = \frac{\gamma}{2\Delta} \int_{\theta-\Delta}^{\theta+\Delta} e^{-j\pi(p-q)\sin(\alpha)} d\alpha, \quad (32)$$

where $t \in \{H, V\}$ and γ denotes propagation path loss between the transmitter and the receiver given by $\gamma = (1 + (\frac{d_s}{d_0})^\alpha)^{-1}$, where the path loss exponent is set as $\alpha = 3.8$, the distance from the transmitter $d_s(m)$, and the reference distance $d_0 = 30 \text{ m}$ [12]. We assume that the transmit antenna is located at an elevation

⁵By considering the case of the macro cellular (tower-mounted) base station, there can be scatterers surrounding the mobile terminals without significant scattering around the base station [24]. In this case, we can jointly service the angular-separated users in distinct annular regions [12].

⁶In Jake's model [25], $a = J_0(2\pi f_D T_s)$ where $J_0(\cdot)$ is the zeroth-order Bessel function and $f_D = \frac{v}{c}$ is the maximum Doppler frequency shift.

of $h = 60m$ and the local scattering ring around the user has radius $d_r = 30m$. Then, the parameters for the channel covariance matrices \mathbf{R}_V and \mathbf{R}_H are given by $\Delta_V = \frac{1}{2}(\arctan(\frac{d_s+d_r}{h}) - \arctan(\frac{d_s-d_r}{h}))$, $\theta_V = \frac{1}{2}(\arctan(\frac{d_s+d_r}{h}) + \arctan(\frac{d_s-d_r}{h}))$, $\Delta_H = \arctan(\frac{d_r}{d_s})$, and $\theta_H \in (-\frac{\pi}{3}, \frac{\pi}{3})$ for a sector in a cell.

A. Practical Guidelines for Training Sequence

In this subsection, a practical guideline for training sequence parameters is developed with quantitative analysis.

First, one can improve channel estimation performance by choosing the row length of \mathbf{C} large enough to incorporate more dominant eigen-directions of the channel in the $G \times M_p$ training sequence. Intuitively, the channel MSE of the $nG \times M_p$ training sequence ($n \in \mathbb{N}$) is *at least* equal to those of the $G \times M_p$ training sequence by n times repetition of the shorter version of the training sequence. Fig. 4 shows the closed-form expressions of the upper and lower bounds in (13) and (15). It is seen that increasing G is indeed beneficial in terms of the channel MSE, but the effect becomes marginal when G is too large. That is, the proposed training sequence can operate on a finite G regime to achieve reasonably good channel estimation performance, which implies that increasing the training period length M_p also has similar effect on the channel MSE due to the increased training sequence size.

Second, though the increased M_p enables large beam-forming gain by leveraging channel estimation performance, an increment of M_p can degrade achievable data rate because the remaining $M - M_p$ channel uses are only available for downlink data transmission. Therefore, we examine the trade-off of spectral efficiency in (30) corresponding to the value of M_p , which was obtained by using Algorithm 1 for simplicity. In Fig. 5, when the value of G is small, the spectral efficiency benefits from the slightly increased M_p since increasing M_p enables the $G \times M_p$ training sequence to incorporate more dominant directions of the channel for channel estimation accuracy. However, increasing M_p over some threshold limits the spectral efficiency due to the shorter length of data transmission period, as expected from the pre-log factor in (30). The tension between channel estimation accuracy and achievable data rate yields that the value of M_p should be properly selected under given system parameters. Instead of this nontrivial choice, we can again increase the (vertical) sequence size G for channel estimation accuracy without affecting the pre-log term. Fig. 5 shows that the increased G makes the spectral efficiency quite insensitive w.r.t. M_p for the practical range of the value of G .

Furthermore, we focus on the optimal number of dimensionality variable n_d^* (or the number of active RF chains in the case of hybrid precoding) obtained from the proposed method. The reduced dimensionality n_d^* used for training sequence and transmit beamforming design provides insight into the (effective) dominant channel rank considered for transmitting multiple data streams or the beamforming gain.

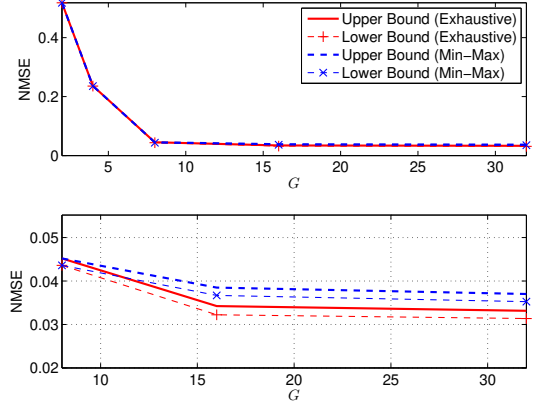


Fig. 4. NMSE versus the training sequence size G where $N_t = 375$, $M = 20$, $M_p = 2$, $N_d = GM_p$, $\rho = 10$, $d_s = 100$, and $v = 3km/h$

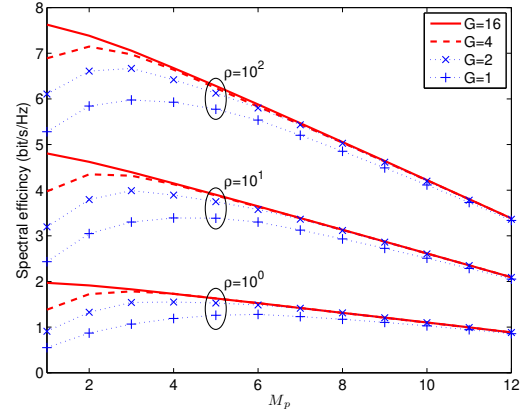


Fig. 5. Spectral efficiency versus training period length M_p where $N_t = 375$, $M = 20$, $N_d = 50$, $d_s = 100$, and $v = 3km/h$

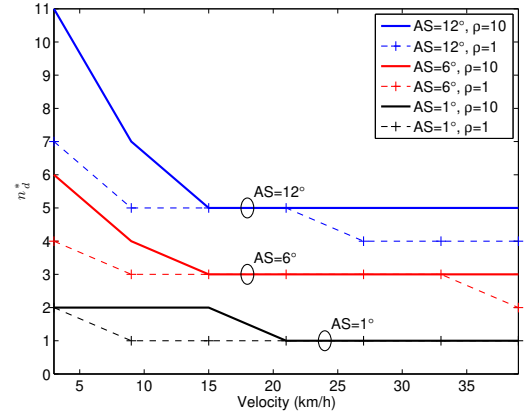


Fig. 6. The optimized value of n_d^* for training sequence and transmit precoding where $N_t = 375$, $M = 20$, $M_p = 1$, $G = 32$, $N_d = 50$, and $d_s = 150$

Fig. 6 shows that, at high SNR, more training beam patterns are used to incorporate sufficient channel gains by subspace sampling in a sufficient broad space. On the other hand, smaller training beam patterns are required to account for the most dominant eigen-directions of the channel, in the low-SNR regime. In addition, the user's mobility also affects the value of n_d^* because the estimated channel is more likely outdated in case of a fast-mobility case. Thus, one can mitigate the channel aging effect on the most dominant

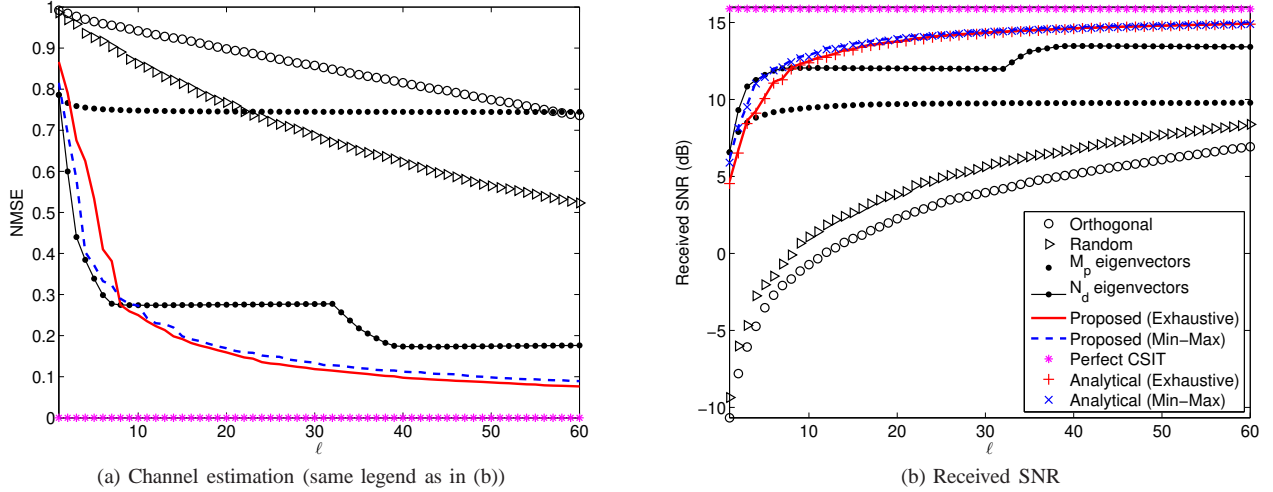


Fig. 7. NMSE and received SNR versus block time index ℓ where $N_t = 375$, $M = 20$, $M_p = 2$, $G = 32$, $N_d = 64$, $\rho = 10$, and $v = 3\text{km/h}$

eigen-directions by properly reducing the dimension of the sampling subspace of the channel, i.e., properly reduce the number of unique training beam patterns n_d . This result indicates the influence of various system parameters such as channel spatial correlation, angular spread, transmit power, and user terminals' mobility on the effective channel rank based on the propose method.

B. Performance Evaluation of Training Techniques

We compared the performance of the proposed methods to those of several downlink training techniques [26]–[28]. For all considered channel sounding methods, we used Kalman filtering for channel estimation. Fig. 7 shows the performance comparison with several training signal design methods [26]–[28] with $N_t = 375$ ($N_V = 15$, $N_H = 25$), $N_d = 64$, $\theta_H = \frac{\pi}{6}$, and $d_s = 100\text{m}$. Orthogonal and random training signals are chosen at the beginning of simulation and used in a round-robin manner. These methods are ineffective in terms of the amount of training duration for achieving reasonable channel estimation accuracy since such training signal patterns cannot effectively capture the dominant channel directions over all the N_t -dimensional space at each training period. The training signal composed of the fixed M_p dominant eigenvectors of \mathbf{R}_h can only minimize the channel MSE in the limited subspace spanned by the fixed M_p training vectors. Thus, the fixed training signal approach saturates quickly. We also consider the modified scheme that initially selects the N_d dominant eigenvectors of \mathbf{R}_h and transmits M_p training signals among the chosen N_d training signal patterns across G consecutive training periods where $N_d = GM_p$. The N_d fixed training scheme shows the best performance up to the initial 7 blocks and becomes inefficient for the remaining duration. This result indicates that about 14 eigen-directions contain the most dominant channel gain which is not known in priori.

The proposed methods with the optimal number of training signal patterns $n_d^* = 24$ substantially reduce the train-

Method	NMSE	Received SNR (dB)
Orthogonal	0.13	13.8
Random	0.13	13.8
M_p eigenvectors	0.74	9.3
N_d eigenvectors	0.05	14.9
Proposed (Exhaustive)	0.03	15.3
Proposed (Min-Max)	0.04	15.3
Proposed (Exhaustive: hybrid)	0.04	15.2
Proposed (Min-Max: hybrid)	0.05	15.2
Perfect CSIT	0.00	15.8

TABLE II
STEADY-STATE PERFORMANCE: COMPARISON OF SEVERAL METHODS

ing duration necessary to achieve good channel estimation accuracy. This yields that the proper use of less dominant eigen-directions of the channel indeed leverages channel estimation performance. Within the first few blocks, the min-max approach in Algorithm 1 shows better performance than the exhaustive approach in Fig. 7(a). This is because the min-max training sequence is designed to sequentially minimize the dominant steady-state channel MSE, thus this approach shows a slightly steeper initial slope on the channel MSE. As a matter of fact, the exhaustive approach will eventually provide the best channel estimation performance, but only a marginal performance difference is observed in comparison with the min-max approach as shown in Table II. The proposed methods outperform other methods over almost all of transmission periods in terms of the channel MSE and the received SNR. Our simulation results also matches the analytic result of (48) very well in Fig. 7(b).

Fig. 8 shows the performance of the proposed hybrid precoding design, where the DFT-based training sequence is used by exploiting the approximated channel spatial correlation \mathbf{R}_h in (21). It is seen that the proposed hybrid precoding method yields almost the same performance as the method with perfectly known \mathbf{R}_h during the transient phase in Fig. 8, and also shows a negligible performance difference in the steady-state phase as shown in Table II. An observation of practical importance is that the proposed

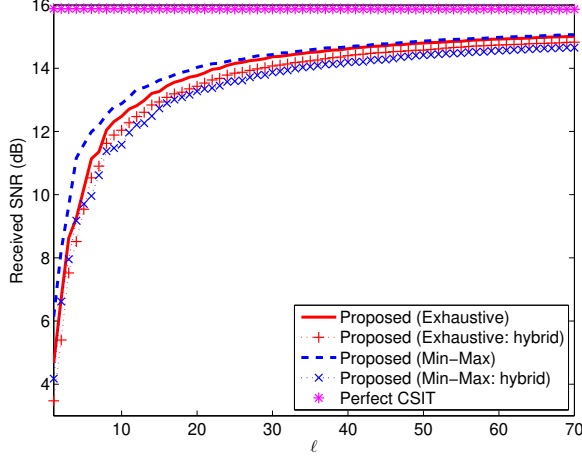


Fig. 8. Received SNR versus block time index ℓ where $N_t = 375$, $M = 5$, $M_p = 2$, $G = 32$, $\rho = 10$, and $v = 3 \text{ km/h}$

hybrid precoding method based on a rough estimation of \mathbf{R}_h by using the DFT vectors seems to work well in FDD massive MIMO systems even with a limited number of RF chains for transmit beamforming.

Finally, we evaluated the proposed method in the multiple-user situation with the ULA ($N_t = 128$) at the base station to service U users in a sector of a cell for the same setup as before. We assume that users are distributed in a sector with $\theta_u = -\frac{\pi}{3} + \Delta + (u-1)\frac{2\pi}{3}\frac{1}{U}$ (angle of arrival of user u) and $\Delta = \arctan(\frac{d_r}{d_s})$ (angular spread) for $d_r = 8$, $d_s = 150$, $1 \leq u \leq U$, and $U = 8$. Here, the SNR is defined as $\gamma\rho$ to account for the signal transmit power and the propagation path loss in (32). Fig. 9 shows that the performance of the lower bound on sum spectral efficiency in (31) under the several parameters of the dimensionality constraints N_d and the terminal velocity. The performance of perfect CSIT case is shown as the performance reference. In Fig. 9, the proposed method achieves close performance of full CSIT with the reasonably increased dimensionality constraint.

VI. CONCLUSION

We considered a reduced dimensionality training sequence and transmit precoding design aimed at enabling low-complexity and energy-efficient system implementation. We have proposed a new method for training sequence design that leverages the steady-state channel estimation performance in conjunction with Kalman filtering. The low-dimensionality constraint on training sequence and transmit precoding extends to a hybrid analog-digital precoding scheme that uses a limited number of active RF chains for transmit precoding by applying the Toeplitz distribution theorem with specific antenna configurations. We derive some necessary conditions to the optimal solution and provide a practical guideline for training sequence parameters with performance analysis. The proposed method can provide a way to realize energy-efficient large-scale antenna systems.

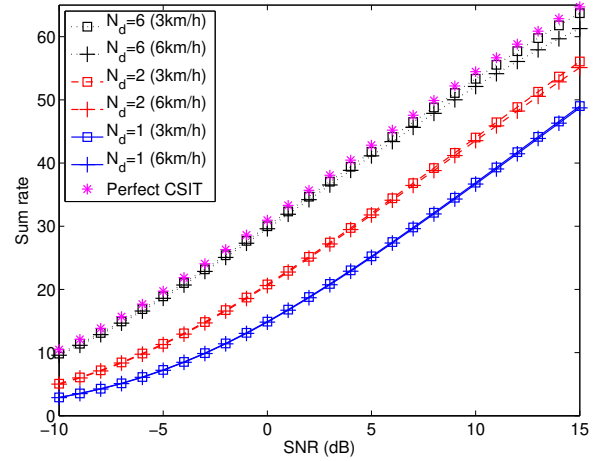


Fig. 9. A lower bound on sum spectral efficiency versus SNR (dB) where $N_t = 128$, $M = 20$, $M_p = 1$, and $G = 32$ in the multi-user case.

APPENDIX

A. Proof of Proposition 2

Given $g_i \geq g'_i = g_i - c$ for some $0 \leq c \leq g_i - 1$, we have

$$\frac{a^{2g_i}}{1 - a^{2g_i}} \leq \frac{a^{2g'_i}}{1 - a^{2g'_i}} = \frac{a^{2g_i}}{1 - a^{2g_i}} \gamma_c, \quad (33)$$

where $\gamma_c := \frac{1 - a^{2g_i}}{a^{2c} - a^{2g_i}} \geq 1$. From (13) and (33), the channel MSE λ_{i,g_i}^∞ is increasing on g_i as

$$\begin{aligned} \lambda_{i,g_i}^{(\infty)} &= \frac{\lambda_i}{\left(\frac{1}{2}(1 + \lambda_i\rho)\right) + \sqrt{\left(\frac{1}{2}(1 + \lambda_i\rho)\right)^2 + \frac{a^{2g_i}}{1 - a^{2g_i}}\lambda_i\rho}} \\ &\geq \frac{\lambda_i}{\left(\frac{1}{2}(1 + \lambda_i\rho)\right) + \sqrt{\left(\frac{1}{2}(1 + \lambda_i\rho)\right)^2 + \frac{a^{2g'_i}}{1 - a^{2g'_i}}\gamma_c\lambda_i\rho}} \\ &= \lambda_{i,g'_i}^{(\infty)} \end{aligned}$$

In (15), $\lambda_{i,g_i}^{(\infty)}$ is a convex combination of $\lambda_{i,g_i}^{(\infty)}$ and λ_i satisfying $\lambda_{i,g_i}^{(\infty)} < \lambda_i$ and thereby an increasing function as g_i increases. Since the composite of increasing functions is increasing:

$$\begin{aligned} \lambda_{i,g'_i}^{(\infty)} &= a^{2(g'_i-1)}\lambda_{i,g'_i}^{(\infty)} + (1 - a^{2(g'_i-1)})\lambda_i \\ &\leq a^{2(g_i-1)}\lambda_{i,g'_i}^{(\infty)} + (1 - a^{2(g_i-1)})\lambda_i \\ &\leq a^{2(g_i-1)}\lambda_{i,g_i}^{(\infty)} + (1 - a^{2(g_i-1)})\lambda_i = \lambda_{i,g_i}^{(\infty)}, \end{aligned}$$

then we have the claim. \blacksquare

B. Proof of Corollary 1

Proof is by induction, where the notations follows those of Step (1) and Step (2). When $q = 1$, let $U_j = G = p^s$ be the initial value for $1 \leq j \leq M_p$ where given $\{g_1, \dots, g_{n_d}\} \in \mathcal{I}_G = \{1, p, \dots, p^s\}$ as in (10). For any $1 \leq q \leq G$, if $U_j \neq 0$, suppose that the unused U_j entries at the j -th column can be described by the n_j disjoint sets of equi-spacing $g_{i,q,j} = p^{k_{i,q,j}} \in \mathcal{I}_G$, i.e., $U_j = n_j \cdot p^{s-k_{i,q,j}}$ for some nonnegative integers n_j and $k_{i,q,j}$. This means that the unused U_j entries

can be viewed as a collection of n_j disjoint sets where the entries of each set are equi-spaced with $g_{i_{q,j}} = p^{k_{i_{q,j}}}$. Thus, after inserting the index of $i_{q,j}$ with a row-wise allocation at Step (I), U_j is updated as $U_j = (n_j - 1) \cdot p^{s-k_{i_{q,j}}}$.

In the subsequent iteration, if $U_j \neq 0$, there exist some row index $q' > q$ such that we need to allocate the index of $i_{q',j}$ using a row-wise mapping $g_{i_{q',j}}$ starting from $[\mathbf{C}]_{q',j}$ as shown in (19). Note that, by the assumption, it follows that $g_{i_{q',j}} \geq g_{i_{q,j}}$. Since each set of equi-spacing $g_{i_{q,j}} = p^{k_{i_{q,j}}}$ at the preceding step can be separated by the $g_{i_{q',j}}/g_{i_{q,j}} = p^{k_{i_{q',j}}-k_{i_{q,j}}}$ disjoint subsets of equi-spacing $g_{i_{q',j}} = p^{k_{i_{q',j}}}$, the remaining U_j entries can be viewed as the $(n_j - 1)p^{k_{i_{q',j}}-k_{i_{q,j}}}$ disjoint sets of equi-spacing $g_{i_{q',j}}$, i.e., $U_j = ((n_j - 1)p^{k_{i_{q',j}}-k_{i_{q,j}}}) \cdot p^{s-k_{i_{q',j}}}$. Therefore, it is possible to allocate the index of $i_{q',j}$ into one of the disjoint sets of equi-spacing $g_{i_{q',j}}$. We then update $n_j = (n_j - 1)p^{k_{i_{q',j}}-k_{i_{q,j}}}$ and $U_j = (n_j - 1) \cdot p^{s-k_{i_{q',j}}}$. Since this process repeats until $U_j \neq 0$ for all j , we have the claim. ■

Lemma 1: During the ℓ -th training period, the channel estimate $\hat{\mathbf{h}}_{u,\ell|\ell}$ based on Kalman filtering is characterized by $E\{\hat{\mathbf{h}}_{u,\ell|\ell}\} = \mathbf{0}$ and $E\{\hat{\mathbf{h}}_{u,\ell|\ell}\hat{\mathbf{h}}_{u,\ell|\ell}^H\} = \mathbf{R}_{\mathbf{h}_u} - \mathbf{P}_{u,\ell|\ell}$.

Proof: For notational simplicity, we omit the lower index u . From (5) and (6), the channel estimate $\hat{\mathbf{h}}_{\ell|\ell}$ for $\ell = 0$ is given by

$$\hat{\mathbf{h}}_{0|0} = \mathbf{P}_{0|-1}\mathbf{S}_0(\mathbf{S}_0^H\mathbf{P}_{0|-1}\mathbf{S}_0 + \mathbf{I}_{M_p})^{-1}\mathbf{y}_{0,pilot}, \quad (34)$$

where recall that $\mathbf{y}_{\ell,pilot} = [y_{\ell M+1}, \dots, y_{\ell M+M_p}]^T$ denotes the ℓ -th received training symbols and $\mathbf{S}_{u,\ell} = [\mathbf{s}_{u,\ell M+1} \dots \mathbf{s}_{u,\ell M+M_p}]$ denotes the ℓ -th training symbols, as shown in (4). Since $E\{\mathbf{y}_{0,pilot}\mathbf{y}_{0,pilot}^H\} = \mathbf{S}_0^H\mathbf{P}_{0|-1}\mathbf{S}_0 + \mathbf{I}_{M_p}$, we have

$$\begin{aligned} E\{\hat{\mathbf{h}}_{0|0}\hat{\mathbf{h}}_{0|0}^H\} &= \mathbf{P}_{0|-1}\mathbf{S}_0(\mathbf{S}_0^H\mathbf{P}_{0|-1}\mathbf{S}_0 + \mathbf{I}_{M_p})^{-1}\mathbf{S}_0^H\mathbf{P}_{0|-1} \\ &\stackrel{(a)}{=} \mathbf{R}_{\mathbf{h}} - (\mathbf{P}_{0|-1} - \mathbf{P}_{0|-1}\mathbf{S}_0 \\ &\quad (\mathbf{S}_0^H\mathbf{P}_{0|-1}\mathbf{S}_0 + \mathbf{I}_{M_p})^{-1}\mathbf{S}_0^H\mathbf{P}_{0|-1}) \\ &= \mathbf{R}_{\mathbf{h}} - \mathbf{P}_{0|0}, \end{aligned}$$

where (a) holds by $\mathbf{P}_{0|-1} = \mathbf{R}_{\mathbf{h}}$ in (5). Note that $E\{\hat{\mathbf{h}}_{0|0}\} = \mathbf{0}$ from $E\{\mathbf{y}_{0,pilot}\} = \mathbf{S}_0^HE\{\mathbf{h}_0\} + E\{\mathbf{w}_0\} = \mathbf{0}$.

During the ℓ -th training period for $\ell \in \mathbb{N}$, the channel estimate $\hat{\mathbf{h}}_{\ell|\ell}$ is given by from (6) and (8):

$$\begin{aligned} \hat{\mathbf{h}}_{\ell|\ell} &= a\hat{\mathbf{h}}_{\ell-1|\ell-1} + \mathbf{P}_{\ell|\ell-1}\mathbf{S}_{\ell}(\mathbf{S}_{\ell}^H\mathbf{P}_{\ell|\ell-1}\mathbf{S}_{\ell} + \mathbf{I}_{M_p})^{-1} \\ &\quad (\mathbf{y}_{\ell,pilot} - \mathbf{S}_{\ell}^Ha\hat{\mathbf{h}}_{\ell-1|\ell-1}). \end{aligned} \quad (35)$$

Denote by $\mathbf{e}_{\ell} \in \mathbb{C}^{M_p}$ the innovation process of Kalman filter

given by

$$\mathbf{e}_{\ell} = \mathbf{y}_{\ell,pilot} - \mathbf{S}_{\ell}^H(a\hat{\mathbf{h}}_{\ell-1|\ell-1}) \quad (36)$$

$$= (\mathbf{S}_{\ell}^H\mathbf{h}_{\ell} + \mathbf{w}_{\ell}) - \mathbf{S}_{\ell}^H(a\hat{\mathbf{h}}_{\ell-1|\ell-1}) \quad (37)$$

$$\begin{aligned} &= (\mathbf{S}_{\ell}^H(a(\hat{\mathbf{h}}_{\ell-1|\ell-1} + \tilde{\mathbf{h}}_{\ell-1}) + \sqrt{1-a^2}\mathbf{b}_{\ell}) + \mathbf{w}_{\ell}) \\ &\quad - \mathbf{S}_{\ell}^Ha\hat{\mathbf{h}}_{\ell-1|\ell-1} \end{aligned} \quad (38)$$

$$= \mathbf{S}_{\ell}^H(a\tilde{\mathbf{h}}_{\ell-1} + \sqrt{1-a^2}\mathbf{b}_{\ell}) + \mathbf{w}_{\ell}, \quad (39)$$

where the equality (38) holds by (2) and $\tilde{\mathbf{h}}_{\ell} := \mathbf{h}_{\ell} - \hat{\mathbf{h}}_{\ell|\ell}$. Note that \mathbf{e}_{ℓ} is independent of $\hat{\mathbf{h}}_{\ell-1|\ell-1}$ due to the orthogonality property of the MMSE estimation and an independent process noise \mathbf{b}_{ℓ} , then we have that \mathbf{e}_{ℓ} has zero mean and covariance matrix $E\{\mathbf{e}_{\ell}\mathbf{e}_{\ell}^H\} = \mathbf{S}_{\ell}^H\mathbf{P}_{\ell|\ell-1}\mathbf{S}_{\ell} + \mathbf{I}_{M_p}$. Thus, we obtain $E\{\hat{\mathbf{h}}_{\ell|\ell}\} = aE\{\hat{\mathbf{h}}_{\ell-1|\ell-1}\} + \mathbf{K}_{\ell}E\{\mathbf{e}_{\ell}\} = \mathbf{0}$. From (35), $E\{\hat{\mathbf{h}}_{\ell|\ell}\hat{\mathbf{h}}_{\ell|\ell}^H\}$ is given by

$$\begin{aligned} &E\{\hat{\mathbf{h}}_{\ell|\ell}\hat{\mathbf{h}}_{\ell|\ell}^H\} \\ &= a^2E\{\hat{\mathbf{h}}_{\ell-1|\ell-1}\hat{\mathbf{h}}_{\ell-1|\ell-1}^H\} + \mathbf{K}_{\ell}E\{\mathbf{e}_{\ell}\mathbf{e}_{\ell}^H\}\mathbf{K}_{\ell}^H \end{aligned} \quad (40)$$

$$\begin{aligned} &= a^2(\mathbf{R}_{\mathbf{h}} - \mathbf{P}_{\ell-1|\ell-1}) \\ &\quad + (\mathbf{P}_{\ell|\ell-1}\mathbf{S}_{\ell}(\mathbf{S}_{\ell}^H\mathbf{P}_{\ell|\ell-1}\mathbf{S}_{\ell} + \mathbf{I}_{M_p})^{-1}\mathbf{S}_{\ell}^H\mathbf{P}_{\ell|\ell-1}) \end{aligned} \quad (41)$$

$$\begin{aligned} &= a^2\mathbf{R}_{\mathbf{h}} - (\mathbf{P}_{\ell|\ell-1} - (1-a^2)\mathbf{R}_{\mathbf{h}}) \\ &\quad + (\mathbf{P}_{\ell|\ell-1}\mathbf{S}_{\ell}(\mathbf{S}_{\ell}^H\mathbf{P}_{\ell|\ell-1}\mathbf{S}_{\ell} + \mathbf{I}_{M_p})^{-1}\mathbf{S}_{\ell}^H\mathbf{P}_{\ell|\ell-1}) \end{aligned} \quad (42)$$

$$\begin{aligned} &= \mathbf{R}_{\mathbf{h}} - (\mathbf{P}_{\ell|\ell-1} - \mathbf{P}_{\ell|\ell-1}\mathbf{S}_{\ell}(\mathbf{S}_{\ell}^H\mathbf{P}_{\ell|\ell-1}\mathbf{S}_{\ell} + \mathbf{I}_{M_p})^{-1} \\ &\quad \mathbf{S}_{\ell}^H\mathbf{P}_{\ell|\ell-1}) \end{aligned} \quad (43)$$

$$= \mathbf{R}_{\mathbf{h}} - \mathbf{P}_{\ell|\ell}, \quad (44)$$

where the equality (42) follows (8). Since this Kalman recursion repeats, we have the claim. ■

C. Proof of Proposition 3

To derive the deterministic quantity for $SINR_{u,\ell}$ in the limit of $N_t \rightarrow \infty$, we use the analysis technique [6]. Applying Lemma 1, we have

$$\frac{1}{N_t^2}|\hat{\mathbf{h}}_{u,\ell|\ell}^H\hat{\mathbf{h}}_{u,\ell|\ell}|^2 - \frac{1}{N_t^2}|\text{tr}(\mathbf{R}_{\mathbf{h}_u} - \mathbf{P}_{u,\ell|\ell})|^2 \xrightarrow[N_t \rightarrow \infty]{a.s.} 0, \quad (45)$$

where $\xrightarrow[N_t \rightarrow \infty]{a.s.}$ denotes the almost sure convergence. If $u \neq u'$, then $\mathbf{h}_{u,\ell}$ and $\hat{\mathbf{h}}_{u',\ell|\ell}$ are mutually independent, thus we have using Lemma 1 as

$$\frac{1}{N_t^2}|\mathbf{h}_{u,\ell}^H\hat{\mathbf{h}}_{u',\ell|\ell}|^2 - \frac{1}{N_t^2}\text{tr}(\mathbf{R}_{\mathbf{h}_u}(\mathbf{R}_{\mathbf{h}_{u'}} - \mathbf{P}_{u',\ell|\ell})) \xrightarrow[N_t \rightarrow \infty]{a.s.} 0, \quad (46)$$

Since $\tilde{\mathbf{h}}_{u,\ell}$ is independent of $\hat{\mathbf{h}}_{u',\ell|\ell}$ for $u \neq u'$ by the orthogonality property of the MMSE estimate, we obtain by using Lemma 1 and $\tilde{\mathbf{h}}_{u',\ell|\ell} \sim \mathcal{CN}(\mathbf{0}, \mathbf{P}_{u',\ell|\ell})$ as

$$\frac{1}{N_t^2}|\tilde{\mathbf{h}}_{u,\ell}^H\hat{\mathbf{h}}_{u',\ell|\ell}|^2 - \frac{1}{N_t^2}\text{tr}(\mathbf{P}_{u,\ell|\ell}(\mathbf{R}_{\mathbf{h}_{u'}} - \mathbf{P}_{u',\ell|\ell})) \xrightarrow[N_t \rightarrow \infty]{a.s.} 0. \quad (47)$$

Substituting (45), (46), and (47) into (25) with $\alpha = (\sum_{u=1}^U \text{tr}(\mathbf{R}_{\mathbf{h}_u} - \mathbf{P}_{u,\ell|\ell}))^{-1}$, we have the deterministic

equivalent SINR, given by

$$\begin{aligned} & \overline{\text{SINR}}_{u,\ell} \\ &= |\text{tr}(\mathbf{R}_{\mathbf{h}_u} - \mathbf{P}_{u,\ell|\ell})|^2 \left(\frac{1}{\alpha\rho} + \text{tr}(\mathbf{P}_{u,\ell|\ell}(\mathbf{R}_{\mathbf{h}_u} - \mathbf{P}_{u,\ell|\ell})) \right) \\ &+ \sum_{u'=1:u' \neq u}^U \text{tr}(\mathbf{R}_{\mathbf{h}_u}(\mathbf{R}_{\mathbf{h}_{u'}} - \mathbf{P}_{u',\ell|\ell})) \Big)^{-1}. \end{aligned} \quad (48)$$

Note that the estimation error covariance matrix $\mathbf{P}_{u,\ell|\ell}$ has the same set of eigenvectors of $\mathbf{R}_{\mathbf{h}_u}$ over all ℓ when we use its eigenvectors as the training signals [9]. That is, given the ED of $\mathbf{R}_{\mathbf{h}_u} = \mathbf{U}_u \mathbf{\Lambda}_u \mathbf{U}_u^H$, $\mathbf{P}_{u,\ell|\ell}$ is eigen-decomposed by $\mathbf{P}_{u,\ell|\ell} = \mathbf{U}_u \bar{\mathbf{\Lambda}}_u^{(\ell)} \mathbf{U}_u^H$. From $\text{tr}(\mathbf{ABC}) = \text{tr}(\mathbf{BCA})$, the terms in (48) are then given by

$$\text{tr}(\mathbf{R}_{\mathbf{h}_u} - \mathbf{P}_{u,\ell|\ell}) = \text{tr}(\mathbf{\Lambda}_u - \bar{\mathbf{\Lambda}}_u^{(\ell)}) \quad (49)$$

$$\text{tr}(\mathbf{R}_{\mathbf{h}_u}(\mathbf{R}_{\mathbf{h}_{u'}} - \mathbf{P}_{u',\ell|\ell})) = \text{tr}(\mathbf{\Lambda}_u \mathbf{U}_u^H \mathbf{U}_{u'} (\mathbf{\Lambda}_{u'} - \bar{\mathbf{\Lambda}}_{u'}^{(\ell)}) \mathbf{U}_{u'}^H \mathbf{U}_u) \quad (50)$$

$$\text{tr}(\mathbf{P}_{u,\ell|\ell}(\mathbf{R}_{\mathbf{h}_{u'}} - \mathbf{P}_{u',\ell|\ell})) = \text{tr}(\bar{\mathbf{\Lambda}}_u^{(\ell)} (\mathbf{\Lambda}_{u'} - \bar{\mathbf{\Lambda}}_{u'}^{(\ell)})) \quad (51)$$

By substituting (49), (50), and (51) into (48), the SINR expression is rewritten as (26). ■

D. Derivation of the lower bound in (31)

By substituting $\mathbf{g}_u \in \mathbb{N}^{n_d}$ into (13) and (15), we can derive $\lambda_{\mathbf{g}_u}^{(\infty)}$ and $\lambda_{\mathbf{g}_u}^{(\infty)}$. From an inequality of (16), it follows that

$$\|\lambda_u - \lambda_{\mathbf{g}_u}^{(\infty)}\|_1 \leq \lim_{\ell \rightarrow \infty} \|\lambda_u - \bar{\lambda}_{\mathbf{g}_u}^{(\ell)}\|_1 \quad (52)$$

$$\lim_{\ell \rightarrow \infty} \|\bar{\lambda}_{\mathbf{g}_u}^{(\ell)} \odot (\lambda_u - \bar{\lambda}_{\mathbf{g}_u}^{(\ell)})\|_1 \leq \|\lambda_{\mathbf{g}_u}^{(\infty)} \odot (\lambda_u - \lambda_{\mathbf{g}_u}^{(\infty)})\|_1,$$

and

$$\begin{aligned} & \lim_{\ell \rightarrow \infty} \text{tr}(\mathbf{\Lambda}_u \mathbf{U}_u^H \mathbf{U}_{u'} (\mathbf{\Lambda}_{u'} - \bar{\mathbf{\Lambda}}_{\mathbf{g}_{u'}}^{(\ell)}) \mathbf{U}_{u'}^H \mathbf{U}_u) \\ & \leq \text{tr}(\mathbf{\Lambda}_u \mathbf{U}_u^H \mathbf{U}_{u'} (\mathbf{\Lambda}_{u'} - \mathbf{\Lambda}_{\mathbf{g}_{u'}}^{(\infty)}) \mathbf{U}_{u'}^H \mathbf{U}_u), \end{aligned} \quad (53)$$

where $\mathbf{P}_{u,\ell|\ell} = \mathbf{U}_u \bar{\mathbf{\Lambda}}_u^{(\ell)} \mathbf{U}_u^H$ with $\bar{\mathbf{\Lambda}}_u^{(\ell)} = \text{diag}(\bar{\lambda}_{\mathbf{g}_u}^{(\ell)})$, $\mathbf{\Lambda}_{\mathbf{g}_{u'}}^{(\infty)} = \text{diag}(\lambda_{\mathbf{g}_{u'}}^{(\infty)})$, and the initial conditions (5). By applying the inequalities (52) and (53) to (26), we obtain the closed-form lower bound on the steady-state SINR, as shown in (31). ■

REFERENCES

- [1] S. Noh, M. D. Zoltowski, and D. J. Love, "Downlink training codebook design and hybrid precoding in FDD massive MIMO systems," in *Proc. IEEE Global Commun. Conf.*, (to be published) Dec. 2014.
- [2] M. D. Renzo, H. Haas, A. Ghayeb, S. Sugiura, and L. Hanzo, "Spatial modulation for generalized MIMO: Challenges, opportunities and implementation," in *Proc. IEEE*, Jan. 2014, vol. 102, pp. 56 – 103.
- [3] T. L. Marzetta, "Noncooperative cellular wireless with unlimited numbers of base station antennas," *IEEE Trans. Wireless Commun.*, vol. 9, no. 11, pp. 3590 – 3600, Nov. 2010.
- [4] F. Rusek, D. Persson, B. K. Lau, E. G. Larsson, O. Edfors, F. Tufveson, and T. L. Marzetta, "Scaling up MIMO: Opportunities and challenges with very large arrays," *IEEE Signal Process. Mag.*, vol. 30, no. 1, pp. 40 – 60, Jan. 2013.
- [5] J. Jose, A. Ashikhmin, T. L. Marzetta, and S. Vishwanath, "Pilot contamination and precoding in multi-cell TDD systems," *IEEE Trans. Wireless Commun.*, vol. 10, no. 8, pp. 2640 – 2651, Aug. 2011.
- [6] J. Hoydis, S. ten Brink, and M. Debbah, "Massive MIMO in the UL/DL of cellular networks: How many antennas do we need?," *IEEE J. Sel. Areas Commun.*, vol. 31, no. 2, pp. 160 – 171, Feb. 2013.
- [7] C. Shepard, H. Yu, N. Anand, L. E. Li, T. L. Marzetta, R. Yang, and L. Zhong, "Argos: Practical many-antenna base stations," in *Proc. MobiCom*, Istanbul, Turkey, Aug. 2012.
- [8] S. Noh, M. D. Zoltowski, Y. Sung, and D. J. Love, "Optimal pilot beam pattern design for massive MIMO systems," in *Proc. Asilomar Conf. on Signal, Syst. and Comput.*, Pacific Grove, CA, Nov. 2013.
- [9] S. Noh, M. D. Zoltowski, Y. Sung, and D. J. Love, "Pilot beam pattern design for channel estimation in massive MIMO systems," *J. Sel. Topics Signal Process.*, to be published. [Online]. Available: <http://arxiv.org/abs/1309.7430>.
- [10] J. Choi, Z. Chance, D. J. Love, and U. Madhow, "Noncoherent trellis coded quantization: A practical limited feedback technique for massive MIMO systems," *IEEE Trans. Commun.*, vol. 61, no. 12, pp. 5016 – 5029, Dec. 2013.
- [11] J. Choi, D. J. Love, and P. Bidigare, "Downlink training techniques for FDD massive MIMO systems: Open-loop and closed-loop training with memory," *IEEE J. Sel. Topics Signal Process.*, to be published. [Online]. Available: <http://arxiv.org/abs/1309.7712>.
- [12] A. Adhikary, J. Nam, J.-Y. Ahn, and G. Caire, "Joint spatial division and multiplexing: The large-scale array regime," *IEEE Trans. Inf. Theory*, vol. 59, no. 10, pp. 6441 – 6463, Oct. 2013.
- [13] A. Adhikary and G. Caire, "Joint spatial division and multiplexing: Opportunistic beamforming and user grouping," *J. Sel. Topics Signal Process.*, to be published. [Online]. Available: <http://arxiv.org/abs/1305.7252>.
- [14] G. Lee and Y. Sung, "A new approach to user scheduling in massive multi-user MIMO broadcast channels," *IEEE Trans. Inf. Theory*, submitted for publication. [Online]. Available: <http://arxiv.org/abs/1403.6931>.
- [15] J. So, D. Kim, Y. Lee, and Y. Sung, "Pilot signal design for massive MIMO systems: A received signal-to-noise-ratio-based approach," *IEEE Signal Process. Lett.*, submitted for publication. [Online]. Available: <http://arxiv.org/abs/1406.3404>.
- [16] L. Tong, B. M. Sadler, and M. Dong, "Pilot-assisted wireless transmissions: General model, design criteria, and signal processing," *IEEE Signal Process. Mag.*, vol. 21, no. 6, pp. 12 – 25, Nov. 2004.
- [17] T. Kailath, A. H. Sayed, and B. Hassibi, *Linear Estimation*, Prentice-Hall, Upper Saddle River, New Jersey, 2000.
- [18] M. Dong, L. Tong, and B. M. Sadler, "Optimal insertion of pilot symbols for transmissions over time-varying flat fading channels," *IEEE Trans. Signal Process.*, vol. 52, no. 5, pp. 1403 – 1418, May 2004.
- [19] U. Grenander and G. Szegö, *Toeplitz Forms and Their Applications*, University of California Press, Berkeley, CA, 1958.
- [20] Y. Sung, H. V. Poor, and H. Yu, "How much information can one get from a wireless ad hoc sensor network over a correlated random field?," *IEEE Trans. Inf. Theory*, vol. 55, no. 6, pp. 2827 – 2847, Jun. 2009.
- [21] A. F. Molisch, "A generic model for MIMO wireless propagation channels in macro- and microcells," *IEEE Trans. Signal Process.*, vol. 52, no. 1, pp. 61 – 71, Jan. 2004.
- [22] A. Forenza, D. J. Love, and R. W. Heath Jr., "Simplified spatial correlation models for clustered MIMO channels with different array configurations," *IEEE Trans. Veh. Technol.*, vol. 56, no. 4, pp. 1924 – 1934, Jul. 2007.
- [23] B. Hassibi and B. M. Hochwald, "How much training is needed in multiple-antenna wireless links?," *IEEE Trans. Inf. Theory*, vol. 49, no. 4, pp. 951 – 963, Apr. 2003.
- [24] D. Shiu and G. J. Foschini and M. J. Gans and J. M. Kahn, "Fading correlation and its effect on the capacity of multi element antenna systems," *IEEE Trans. Commun.*, vol. 48, no. 3, pp. 502 – 513, Mar. 2000.
- [25] W. C. Jakes, *Microwave Mobile Communication*, Wiley, New York, NY, 1974.
- [26] W. Santipach and M. L. Honig, "Optimization of training and feedback overhead for beamforming over block fading channels," *IEEE Trans. Inf. Theory*, vol. 56, no. 12, pp. 6103 – 6115, Dec. 2010.
- [27] F. Kaltenberger, M. Kountouris, D. Gesbert, and R. Knopp, "On the trade-off between feedback and capacity in measured MU-MIMO channels," *IEEE Trans. Wireless Commun.*, vol. 8, no. 9, pp. 4866 – 4875, Sep. 2009.
- [28] J. H. Kotecha and A. M. Sayeed, "Transmit signal design for optimal estimation of correlated MIMO channels," *IEEE Trans. Signal Process.*, vol. 52, no. 2, pp. 546 – 557, Feb. 2004.